AD-A174 997 LIGHT SCATTERING THEORY FOR BUBBLES IN WATER: INVERSE SCATTERING COATED B (U) WASHINGTON STATE UNIV PULLMAN DEPT OF PHYSICS P L MARSTON 17 NOV 86 N00014-86-K-0242 1/1

UNCLASSIFIED F/G 20/6 NL

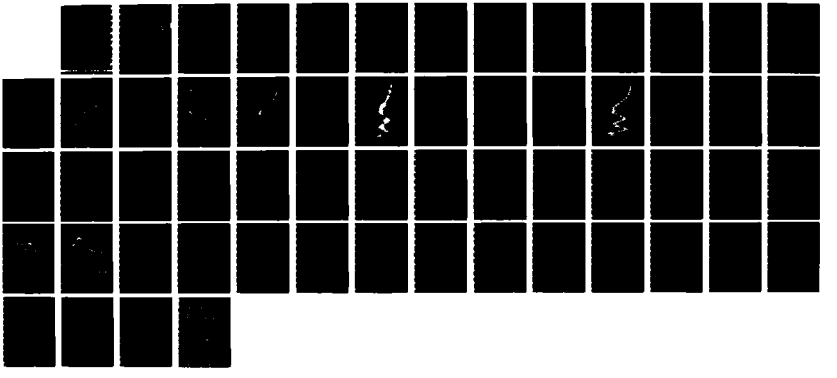

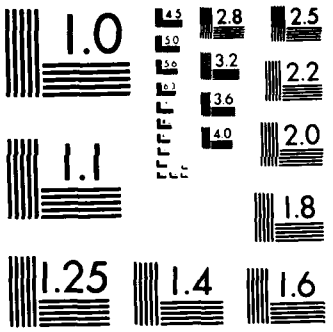

UNCLASSIFIED
SECURITY CLASSIFICATION

(13)

AD-A174 997

DOCUMENTATION PAGE

1a. REPORT SECURITY CLASSIFICATION: UNCLASSIFIED	b. RESTRICTIVE MARKINGS
2a. SECURITY CLASSIFICATION AUTHORITY: N/A since Unclassified	3. DISTRIBUTION/AVAILABILITY OF REPORT: Approved for public release; distribution is unlimited.
2b. DECLASSIFICATION/DOWNGRADING SCHEDULE: N/A since Unclassified	
4. PERFORMING ORGANIZATION REPORT NUMBER(S): N00014-86-K-0242-FR	5. MONITORING ORGANIZATION REPORT NUMBER(S)
6a. NAME OF PERFORMING ORGANIZATION: Washington State University, Department of Physics	6b. OFFICE SYMBOL (If applicable)
6c. ADDRESS (City, State, and ZIP Code): Pullman, WA 99164-2814	7a. NAME OF MONITORING ORGANIZATION: Office of Naval Research Resident Representative, University of Washington
	7b. ADDRESS (City, State, and ZIP Code): 1107 N.E. 45th Street, Seattle, WA 98105-4631
8a. NAME OF FUNDING/SPONSORING ORGANIZATION: Naval Ocean Research & Development Activity	8b. OFFICE SYMBOL (If applicable): NORDA
	9. PROCUREMENT INSTRUMENT IDENTIFICATION NUMBER: N00014-86-K-0242
8c. ADDRESS (City, State, and ZIP Code): Code 331, NSTL, Mississippi 39529-5004	10. SOURCE OF FUNDING NUMBERS

PROGRAM ELEMENT NO.	PROJECT NO.	TASK NO.	WORK UNIT ACCESSION NO.
61153N	03105	330	13316Q

DTIC ELECTE DEC 0 1986 S E

11. TITLE (Include Security Classification): LIGHT SCATTERING THEORY FOR BUBBLES IN WATER: INVERSE SCATTERING, COATED BUBBLES, AND STATISTICS

12. PERSONAL AUTHOR(S): Philip L. Marston

13a. TYPE OF REPORT	13b. TIME COVERED	14. DATE OF REPORT (Year, Month, Day)	15. PAGE COUNT
Final Report	FROM 860201 TO 860930	86 11 17	55

16. SUPPLEMENTARY NOTATION: The telephone number for P. L. Marston, the principal investigator of this contract, is (509) 335-5343 / 335-9531

17. COSATI CODES		
FIELD	GROUP	SUB-GROUP

18. SUBJECT TERMS (Continue on reverse if necessary and identify by block number): Microbubbles, Bubbles, Bubble Detection, Cavitation, Light Scattering, Mie Theory, Inverse Scattering, and Scattering Statistics.

19. ABSTRACT (Continue on reverse if necessary and identify by block number)

Light scattering theory was applied to practical problems related to the detection and sizing of bubbles in ocean water. The emphasis of these calculations was on scattering from microbubbles illuminated by a Gaussian beam into angles close to the critical scattering angle (approximately 83 deg). This emphasis is appropriate for applications to an instrument being developed by NORDA. The specific problems include:

(a) Computational analysis of the effects of surface films on the optical scattering properties of bubbles in water;

(b) Physical optics approximation for the scattering from a coated bubble--explanation of the shift in the coarse structure and polarization effects;

DTIC COPY

20. DISTRIBUTION/AVAILABILITY OF ABSTRACT	21. ABSTRACT SECURITY CLASSIFICATION
☒ UNCLASSIFIED/UNLIMITED ☐ SAME AS RPT. ☐ DTIC USERS	UNCLASSIFIED

22a. NAME OF RESPONSIBLE INDIVIDUAL	22b. TELEPHONE (Include Area Code)	22c. OFFICE SYMBOL
Ming-Yang Su	601-688-5241	NORDA Code 331

DD FORM 1473, 84 MAR — 83 APR edition may be used until exhausted. All other editions are obsolete.

SECURITY CLASSIFICATION OF THIS PAGE: UNCLASSIFIED

19. ABSTRACT (continued)

(c) Brewster-angle scattering from coated and uncoated bubbles: applications to measurement of film thickness and to the discrimination of bubbles from particles;

(d) Detector placement and inversion of scattering data to obtain the bubble size on an event-by-event basis;

(e) Statistical properties of the photodetector voltages and a possible alternative to event-by-event data inversion.

The event-by-event inversion procedure for obtaining the size of each bubble is discussed in an Appendix.

Accession For	
NTIS GRA&I	☒
DTIC TAB	☐
Unannounced	☐
Justification	
By	
Distribution/	
Availability Codes	
Dist	Avail and/or Special
A-1	

LIGHT SCATTERING THEORY FOR BUBBLES IN WATER: INVERSE SCATTERING, COATED BUBBLES, AND STATISTICS

Principal Investigator

Philip L. Marston
Department of Physics
Washington State University
Pullman, WA 99164-2814

FINAL REPORT

February 1, 1986 - September 30, 1986

Contract No. N00014-86-K-0242

(Report No. N00014-86-K-0242-FR)

WORK SPONSORED BY THE NAVAL OCEAN RESEARCH AND DEVELOPMENT ACTIVITY

November 17, 1986

WSU Contract No. 2464-0137

BLANK

TABLE OF CONTENTS

I. EXTERNAL COMMUNICATIONS SUPPORTED BY THIS CONTRACT

A. Reports Issued

1. P. L. Marston, "Progress Report on Research Supported by Contract N00014-86-K0242, Part 1: Detector Placement and Inversion of Light Scattering Data for the Bubble Size Spectrometer of the Wyatt Technology Design" (May 29, 1986).
2. P. L. Marston, "Progress Report on Research Supported by Contract N00014-86-K0242, Part 2: The Effects of Surface Films on Some Optical Scattering Properties of Bubbles in Water" (July 2, 1986).
3. S. C. Billette and P. L. Marston, "Computational Analysis of the Effects of Surface Films on the Optical Scattering Properties of Bubbles in Water," Technical Report issued under contracts N00014-86-K-0242 and N00014-85-C-0141 (October, 1986), Accession Number AD-AXXXXXX(Defense Technical Information Center, Alexandria, VA) 166 pages.

B. Dissertations

1. S. C. Billette, "Computational Analysis of the Effects of Surface Films on the Optical Scattering Properties of Bubbles in Water," thesis submitted in partial fulfillment of the requirements for the degree of Master of Science in Physics, Washington State University, Department of Physics, July 1986.

C. Publications

1. It is planned that a manuscript on "Scattering of light by a coated bubble in water near the critical and Brewster scattering angles," will be submitted to a refereed journal.

D. Oral Presentations and Published Abstracts

1. S. C. Billette and P. L. Marston, "Scattering of light by a coated bubble in water near the critical scattering angle" (abstract only), to appear in J. Opt. Soc. Am. 13 (1986). Presented at the Annual Meeting of the Optical Society of America (Seattle, WA, October 1986).
2. P. L. Marston and S. C. Billette, "Scattering of light by a coated bubble in water near the critical and Brewster scattering angles" (abstract only), J. Acoust. Soc. Am. Suppl. 80, 59 (1986). To be presented at the 112th Meeting of the Acoustical Society of America (Anaheim, CA, Dec. 1986).

E. Other Written Communications

1. Informal progress letter by P. L. Marston to M. Y. Su (dated April 25, 1986).
2. Letter by P. L. Marston to M. Y. Su (dated June 17, 1986) on the generation of microbubbles for calibration purposes.

II. INTRODUCTION AND REVIEW

Previous research (supported by the Office of Naval Research, Physics Division) considered the understanding of the optical scattering properties of microbubbles in water.[1-7] The present research involves the application and extension of that understanding, to recommendations concerning the design and operation of an optical bubble-size spectrometer. The intended instrument would measure the sizes and number densities of bubbles in ocean waters. The data are to be recorded real-time and it would be desirable that the instrument facilitate remote operation. Hence photography of microbubble populations was judged to be unsuitable whereas the electronic recording of optical scattering data from bubbles should, in principle, be invertible to give the desired size measurement. The resources of the present contract ($10,000) were directed entirely

towards theoretical problems of interest for the design and operation of such a spectrometer.

So as to better illustrate the contributions of the present research, it is appropriate to note that the previous research[1-9] used the following three-pronged approach to understanding scattering from bubbles: (i) quantitative and qualitative observations and discovery of new scattering phenomena; (ii) numerical evaluation of partial-wave series (such as the Mie series) which are for special bubble shapes (e.g., uncoated spheres) and comparison of these results with data; (iii) construction and evaluation of simple physical models which are both quantitatively useful and promote understanding. The general motivation for such research is reviewed briefly in Ref. 3, 4, and 6. Recent experiments, carried out here at Washington State University, have emphasized the backscattering of light from bubbles in water.[6,7] Backscattering may be particularly useful if the optical source and detector can not be placed close to the water sample which contains the bubbles.

For the instrument design under consideration by NORDA, however, the optical detectors and source may lie within a few feet (or closer) of the ocean water sample. It appears that the easiest way to measure the size of a bubble with such an instrument is to make use of near critical-angle scattering. This is because the scattering pattern of light from a bubble in water contains broadly spaced structures which are indicative of the bubble radius a. These structures are present as the scattering angle θ (relative to the direction of the incident beam) decreases below the critical value $\theta_c = 82.8°$. The original discovery by Marston of these structures is described in Ref. 9 while a physical-optics approximation (POA) which facilitates a simple understanding is given in Ref. 1-5, 9.

The emphasis of the research supported by the present contract (N00014-86-K-0242) was as follows:

1. Computations that showed how to minimize the effects that natural surface films (on bubbles in the ocean) will have on scattering data--the procedure recommended is to use near-critical-angle scattering data with polarized

incident light with the detectors in the plane of polarization.[10-13] These calculations indicate that there may be an optical method for measuring the film thickness.

2. A method for inversion of bubble scattering data[14,15] on an event-by-event basis--the method is based on placing detectors at the critical scattering angle (θ_c = 82.8 deg) and at several nearby angles $\theta < \theta_c$. The bubbles are assumed to be illuminated by a Gaussian laser beam.
3. Advice given on technical aspects of the design and and testing of an optical bubble spectrometer.[15,16]
4. Preliminary consideration[14] of the statistical properties of the scattering. This may yield a method for inversion of critical-angle scattering data to obtain the size spectrum of a sample of events (in contrast to an event-by-event inversion).

In the present Final Report some aspects of items 1, 2, and 4 will be noted with an emphasis on those results not included in the Technical Report (Ref. 10) previously issued and available from D.T.I.C.

In the Technical Report[10] different values of the refractive index for ocean water had been calculated to have only a weak effect on the relevant scattering properties of the bubbles. Consequently examples displayed in the present report are for water with a refractive index of 4/3 ≈ 1.3333.

III. RESEARCH RESULTS AND ACCOMPLISHMENTS

A. Computational Analysis of the Effects of Surface Films on the Optical Scattering Properties of Bubbles in Water

Many of the unresolved issues concerning microbubbles (of natural origin) in the ocean concern the effects of adsorbed films. Such films are thought to coat most (if not all) bubbles in sea water (see, e.g., Ref. 17). The films should affect the evolution of bubbles

in the sea. Recently published Soviet data,[18] for example, show that the rate at which a bubble shrinks in sea water (when subjected to pressure) is significantly smaller than for bubbles in distilled or tap water. The difference is attributed to the supposed presence of surface films of organic substances. The film "coats" the surface of the gas bubble. Glazman suggests (Sec. I of Ref. 19) that the film thickness may range from 10 nm to 1 μm.

The emphasis of the present research was to examine the influence such films would have on the near critical-angle light scattering pattern for a bubble in water. The issue is important since, if these films were predicted to mask the critical-angle pattern for uncoated bubbles,[1-4,9] it would be necessary to consider major design changes for the proposed bubble-size spectrometer. Fortunately, it was found that the films should have only a minor influence on the scattering pattern provided certain precautions are taken.[10] Of these, the most important are: (1) to make use of the coarse structure in the scattering pattern but to average over the fine structure; and (2) to use monochromatic incident light which is polarized with the electric field parallel to the scattering plane, that is, the plane which contains the detectors.

The method used in the computations was to evaluate the exact partial-wave series solution for the scattering of light from concentric spheres with parameters appropriate for a coated bubble in water. This exact solution, given by Aden and Kerker for use in other scattering problems[20] will be referred to as the Aden-Kerker Series (AKS). One of the important accomplishments of the present research was to develop a reliable computer program for the scattered irradiance as a function of scattering angle θ for the case in which the sphere's inner radius a greatly exceeded the wavelength of light while the coating thickness h is allowed to be much smaller than wavelength. (It appears that such a reliable program was not previously available.) The design, testing, and a listing, of the computer program are summarized in Ref. 10.

The physical situation considered is shown in Fig. 1. Light is incident on a gas filled bubble coated by a film of thickness $h = b - a$ and refractive index n_c. The refractive index of the surrounding liquid (water) is $n_w = 4/3$ while the refractive index of the gas within the bubble is $n_{air} = 1$. Figure 1 also shows various rays reflected from, and/or refracted by, the bubble. Of course the exact AKS is based directly on the formal solution of Maxwell's equations; it does not rely on geometrical optics. Nevertheless, as will be discussed below, the ray diagram is a first step toward understanding the scattering pattern. For comparison, the dashed rays shown are drawn so as to illustrate the case of no coating (which is equivalent to $n_c = n_w$) while the refraction of the solid rays (at the water-coating interface) has been slightly exaggerated from that of the representative case $n_c = 1.5$. This was done so as to show the direction of the deflection of the rays introduced by the typical coating.

For the purposes of evaluating the AKS partial-wave series, the coating index n_c was usually taken to be 1.5 since that is close to the refractive index of many oily organic substances. Calculations[10] for the case $n_c = 1.45$ and 1.55 were qualitatively similar to those for $n_c = 1.5$ and the quantitative differences may be explained in terms of the simple approximation given in the next section. The scattered irradiances were normalized to the irradiance reflected from a perfectly reflecting sphere having the same radius a as that of the gas pocket within the bubble.[10]

Figure 2 shows the normalized irradiance for the case E-field parallel to the scattering plane. The bubble radius is held constant at $a = 7.5$ μm which corresponds to a size parameter $ka = 100$ (see Ref. 10). The parameter AOB mentioned in the caption is the ratio a/b. Figure 2(a) shows the result for an uncoated bubble; the coarse structure (which gives a minimum in this case at 60 deg.) is clearly seen for $\theta < \theta_c = 82.8$ deg. Figures 2(b) - (e) show the increase in the fine structure amplitude which occurs as the coating thickness $h = b - a$ increases. Even for the relatively thick coatings, Fig. 2(f) - (i), the coarse structure is clearly evident and is similar in appearance to that in Fig. 2(a).

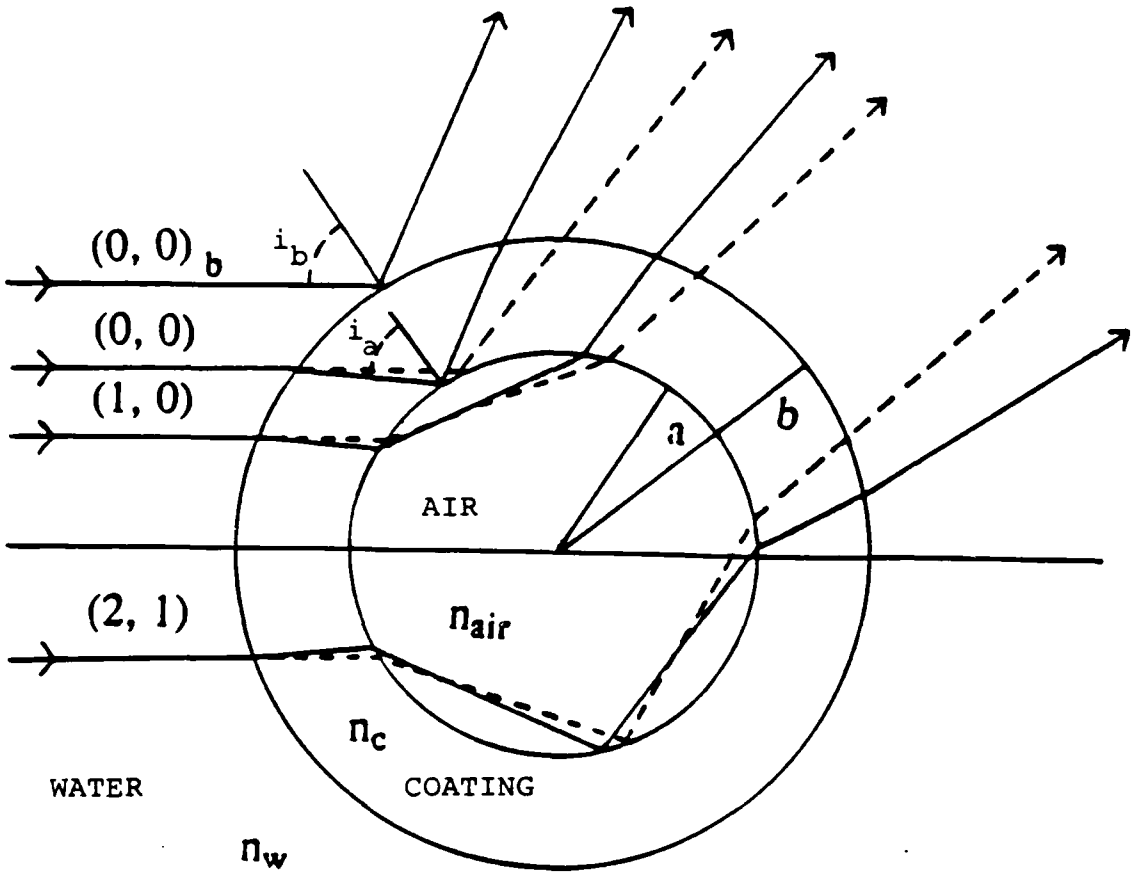

Figure 1. Coated sphere geometric model. Rays are specified by (p,*l*) where p = the number of chords within the bubble, and *l* = the number of crossings of the optic axis. Dashed lines indicate the uncoated sphere ray paths while solid lines represent coated sphere ray paths. Note that bending of the rays is exaggerated for effect. The subscript b indicates rays which pertain to the outer sphere only.

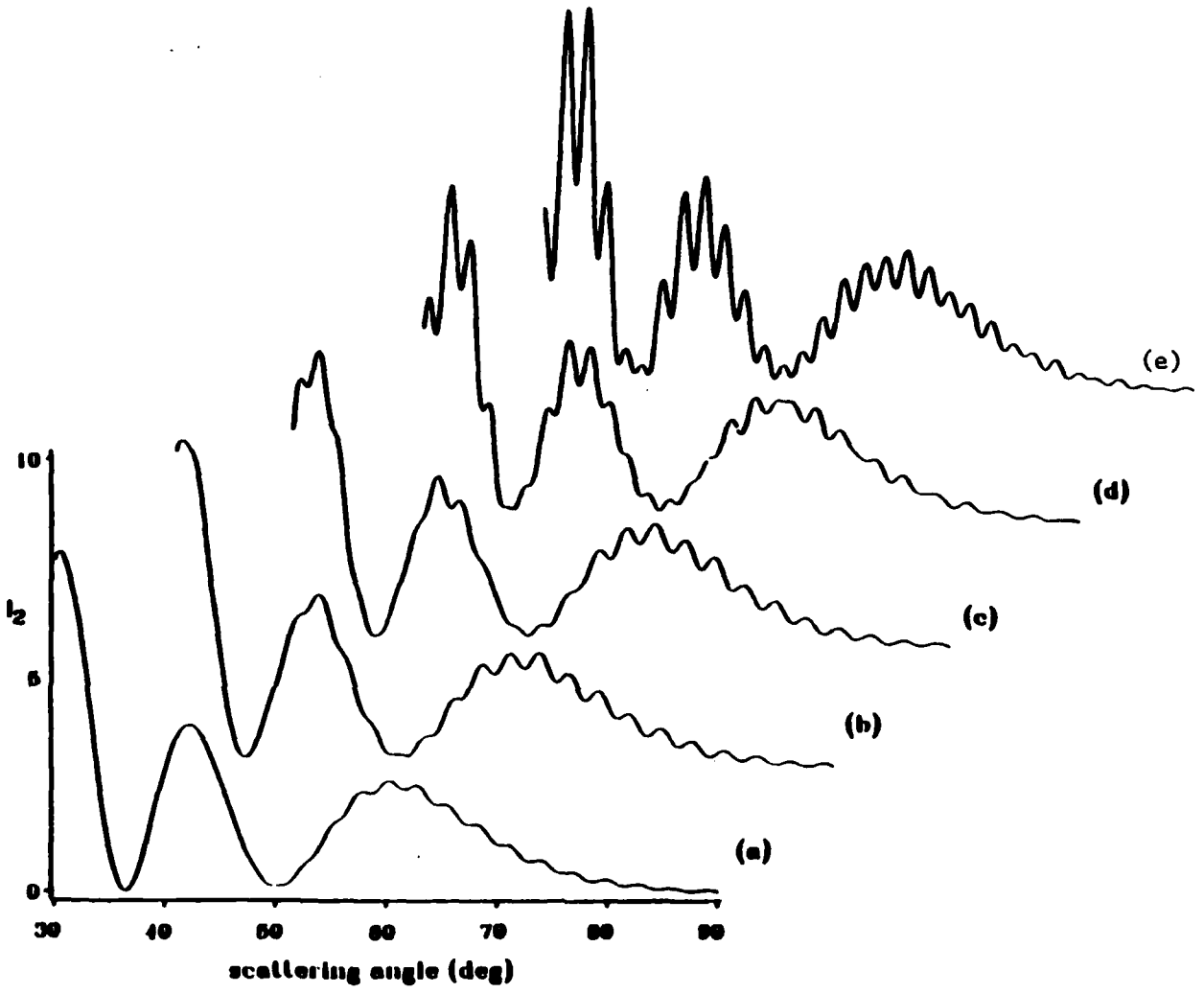

Figure 2. **Evolution of the fine structure as a function of coating thickness for parallel polarized irradiance for ka = 100. Coating thickness values for λ_{air} = 632.8 nm are (a) 0 μm, (b) 0.08 μm, (c) 0.15 μm, (d) 0.19 μm, (e) 0.23 μm, (f) 0.48 μm, (g) 0.66 μm, (h) 0.93 μm, and (i) 1.13 μm. The corresponding values of AOB specified in the computation were: (a) 1.0, (b) 0.990, (c) 0.980, (d) 0.975, (e) 0.970, (f) 0.940, (g) 0.920, (h) 0.890, (i) 0.870.** The scattering angle runs from 30 to 90 deg.

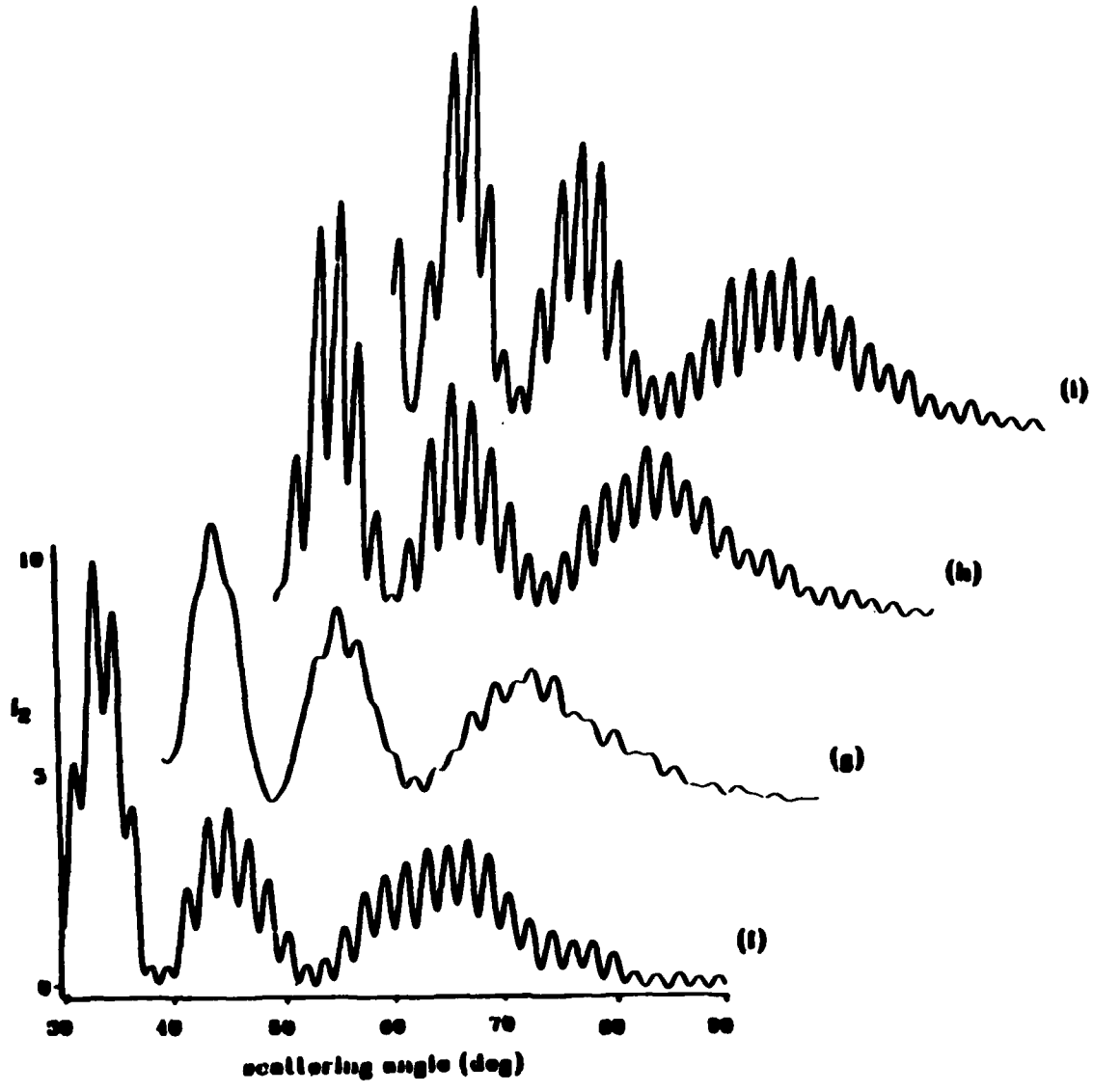

Figure 2(f), (g), (h), and (i).

Figure 3 is like the case shown in Figure 2 except that the full angle range of 0 to 180 deg is shown. The coarse structure is clearly broader in width (and easier to detect) than the relatively narrow forward diffraction lobes. Indeed, if instead of $a = 7.5\ \mu m$ we take $a \approx 75.5\ \mu m$, the angular quasi-period of the forward diffraction lobes decreases by a factor of 10 while the coarse quasi-period decreases by a factor $\cong 3$; consequently, the difference in quasiperiods is even more clearly seen for larger bubbles. Inspection of Fig. 3(b) shows that for this case where h/a has a relatively large value ($1.1/7.5 \approx 0.15$) the coarse structure manifests a noticeable shift towards larger scattering angles.

Figure 4 shows the scattered irradiance for polarized light also for a case in which the E field is parallel to (i.e., lies within) the plane of scattering. In all of the curves $a = 37.8\ \mu m$. The solid curve is for a coated bubble with $h = 1\ \mu m$ and was given by the exact AKS partial-wave series. The curve with short dashes is for an uncoated bubble and was given by the Mie series. These numerical values for h and a are for the case of red light having a wavelength in air of 633 nm. The slowly varying curve with intermediate length dashes is the result of the previous physical-optics approximation (POA) for scattering from a homogeneous bubble previously formulated by Marston and Kingsbury.[1,2] That curve is seen to approximate the coarse structure in the Mie curve (as well as the data for scattering from uncoated bubbles, see Ref. 5). The right-most smooth curve (which alternates a long dash with a short dash) is a shifted plot of the POA curve. That shift was calculated geometrically by Marston so as to obtain an approximate description of the scattering from a coated bubble near the critical scattering angle.

Figure 4 shows that the principal effect of the coating on the coarse structure is to shift slightly its angular location in the direction of increased scattering angle. Notice, however, the coarse structure should not be masked by the presence of the coating. Hence size spectrometers which make use of the coarse structure should still function if the bubble is coated. The coating may, however, introduce a small error (or shift) in the bubble size estimated from scattering data. It is noteworthy that the effects of the coating on the

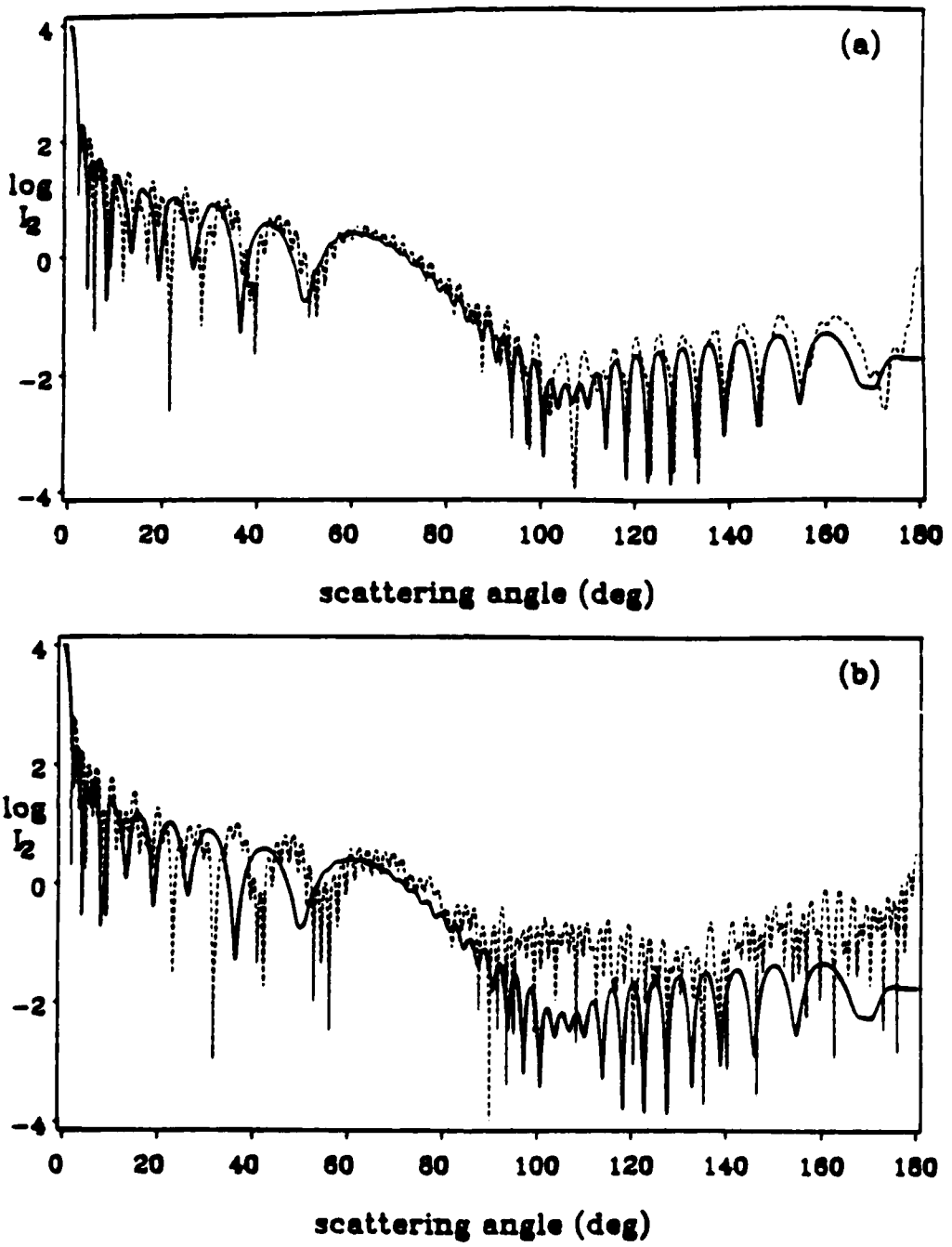

Figure 3. Calculated normalized scattering irradiances I_2 for ka = 100, $n_w = 4/3$, n_c = 1.5, $\theta = 0°$ to 180° for the log of the parallel polarization. The solid curve is from Mie theory. The thin-dashed curve is the calculated coated sphere result for (a) h = 0.26 μm, (b) h = 1.14 μm. All values of h are for HeNe laser light in water with λ_{air} = 632.8 nm. The inner radius a = 7.5 μm.

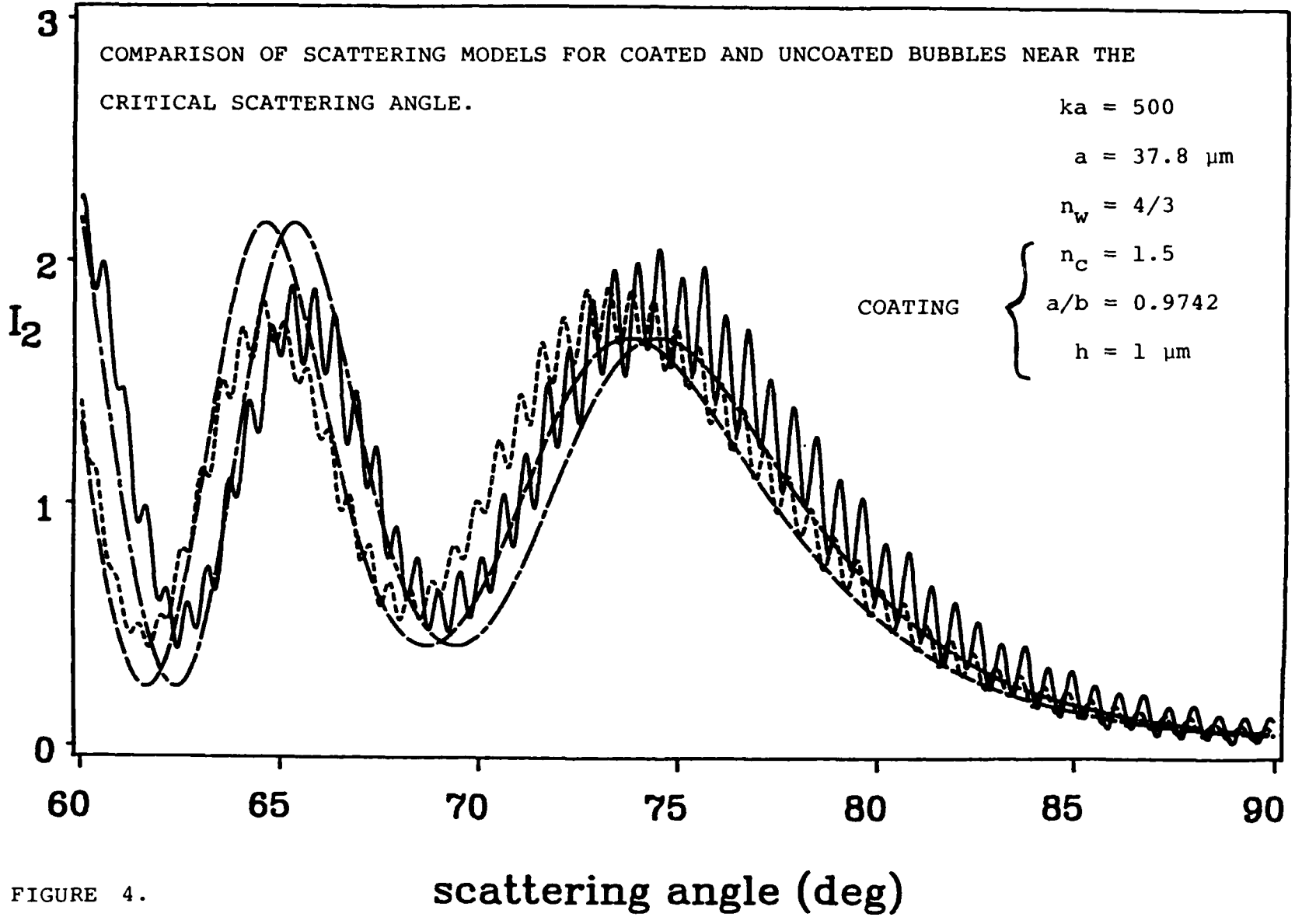
COMPARISON OF SCATTERING MODELS FOR COATED AND UNCOATED BUBBLES NEAR THE CRITICAL SCATTERING ANGLE.
ka = 500
a = 37.8 μm
n_w = 4/3
COATING
n_c = 1.5
a/b = 0.9742
h = 1 μm
I_2
0
1
2
3
60
65
70
75
80
85
90
scattering angle (deg)

FIGURE 4.

orthogonal polarization (E-field perpendicular to the scattering lane) were much more significant; that choice of polarization may be unsuitable for use in a size spectrometer. These polarization effects may be explained in terms of physical arguments.[10]

Figure 5 is for the same radius and coating thickness as Fig. 4 but it shows the normalized irradiance for the case in which the E-field is perpendicular to the plane of scattering. The dashed curve is the case of an uncoated bubble and is given by Mie theory while the solid curve is the coated bubble and is given by the AKS. The effect of the coating on the coarse structure is more than that of the shift evident in Fig. 4.

The Technical Report (Ref. 10) presents computed irradiance plots for bubbles having radii as large as 189 μm. The effects of optical absorption by the coating material were also explored. It turns out that unless the coating contains a dye, absorption should not have a major effect. This is because of the small thickness ($h \leq 1$ μm) of the anticipated films. As noted in the supplement at the end of that report, some of POA (physical optics approximation) plots presented were subject to small computational errors. These errors were subsequently corrected and are not present in the POA plot shown here in Fig. 4.

B. Physical Optics Approximation for the Scattering from a Coated Bubble--Explanation of the Shift in the Coarse Structure and Polarization Effects

Figures 3 and 4 show that the coating shifts the coarse structure to larger scattering angles. To understand this shift, it is appropriate to recall the physical origin of the coarse structure in the physical-optics approximation for the case of an uncoated bubble.[1,2,9] The structure arises because of: (a) the effects of diffraction on the wavefront reflected in the vicinity of the critical angle of incidence, and (b) the interference pattern of the wavefront associated with transmitted rays (predominantly the one-chord ray) with the reflected wavefront. Diffraction is particularly significant when calculating the scattering amplitude associated with the reflected wavefront (a) because of the abrupt drop-off of the local

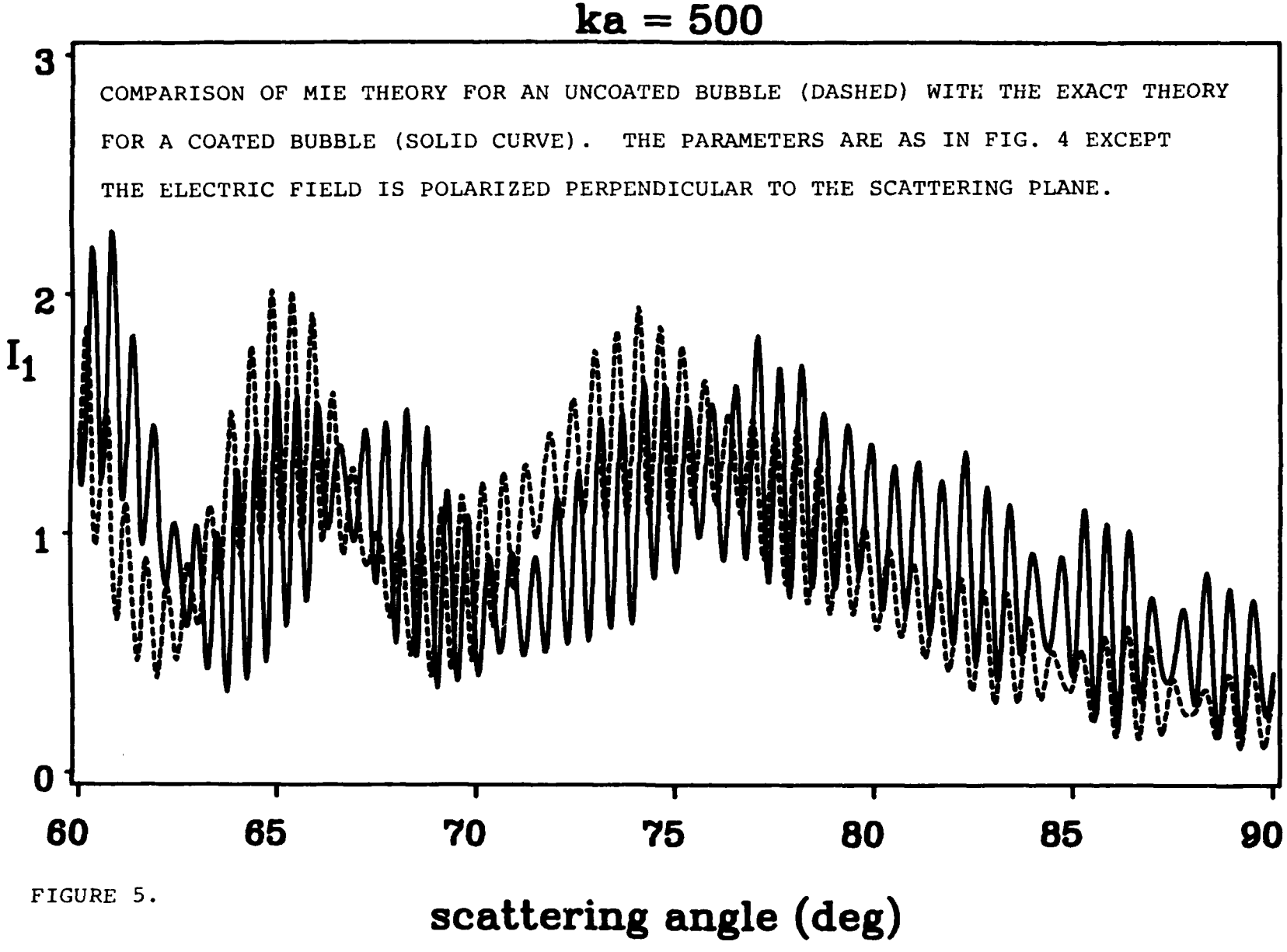
ka = 500
COMPARISON OF MIE THEORY FOR AN UNCOATED BUBBLE (DASHED) WITH THE EXACT THEORY
FOR A COATED BUBBLE (SOLID CURVE). THE PARAMETERS ARE AS IN FIG. 4 EXCEPT
THE ELECTRIC FIELD IS POLARIZED PERPENDICULAR TO THE SCATTERING PLANE.
3
2
1
0
I_1
60
65
70
75
80
85
90
scattering angle (deg)

FIGURE 5.

reflection coefficient as the angle of incidence i falls below the critical value i_c = $\sin(n_w^{-1})$. For the uncoated bubble this reduction occurs when the scattering angle θ is increased above the critical value θ_c

$$\theta_c = \pi - 2i_c = \pi - \sin^{-1}(n_w^{-1}) \cong 82.8° \quad (1)$$

The diffraction and interference patterns caused by effects (a) and (b) are present in the region $\theta < \theta_c$. These patterns have about the same quasi-period and they manifest themselves as the coarse structure in Fig. 2(a) and in the Mie curve in Fig. 4. The interference of the aforementioned ray amplitudes with that of the far-side ray, labeled (2,1) in Fig. 1, gives rise to the fine structure. We will limit our attention to the coarse structure since it is to be used to determine the size of the bubble.

Now what happens when you coat the bubble? The relevant interface at which there is an abrupt transition to total reflection becomes the inner surface of the coating. Denote the local angle of incidence for a ray at this surface by i_a where the subscript a denotes the radius of the relevant interface. There will be an abrupt transition to total reflection here when $i_a \geq i_{ca}$ where the new critical angle is

$$i_{ca} = \sin^{-1}(n_c^{-1}). \quad (2)$$

Now the ray which reflects from the inner surface will be refracted by the coating-water interface and leaves the bubble with a well defined scattering angle relative to the direction of the incident beam. For that ray having $i_a = i_{ca}$, denote the resulting scattering angle by θ_c'. Evidently θ_c' is the critical scattering angle of the coated bubble. The presence of the coating shifts the critical scattering angle by an amount

$$\theta_c' - \theta_c = \Delta, \quad (3)$$

Now Δ is a function of the coating-thickness to radius ratio h/a as well as n_w and n_c. Exact calculation of Δ requires the solution of a set of transcendental equations; however,

Marston obtained the leading term in a power series expansion of $\Delta(h/a)$. The resulting approximation is

$$\Delta = \frac{2h}{a}\left[(n_w^2 - 1)^{-1/2} - (n_c^2 - 1)^{-1/2}\right] + O(h/a)^2, \tag{4}$$

where $O(h/a)^2$ is a function which vanishes as rapidly as $(h/a)^2$ as $h \to O$. The derivation of Eq. (4) was repeated by Cleon Dean, a graduate student partially supported by this contract. Notice that $\Delta \to O$ if the coating index $n_c \to n_w$ or if the thickness $h \to O$.

To approximate the effects of the coating on the coarse structure, the POA for an uncoated bubble may be evaluated with the angular argument shifted by Δ. Let $I_j^{POA}(\theta,ka)$ be the normalized irradiance at scattering angle θ as calculated (for polarization j) by the original POA for an uncoated bubble.[1,2,5] The resulting approximation for the scattering from a coated bubble is

$$I_j^{CPOA}(\theta,ka) \approx I_j^{POA}(\theta - \Delta, ka), \tag{5}$$

where the coating parameters n_c and h/a enter into this approximation only through the approximation of Δ by the first term in Eq. (4). The main idea behind Eq. (5) is that the principal effect of a thin coating (at least for polarization $j = 2$ as noted below) is to shift the scattering angles of the critical ray and the single-chord ray in Fig. 1 by similar amounts. This shift results in a corresponding shift of the diffraction and interference pattern.

How well does Eq. (5) do in approximating the exact AKS results? Consider first polarization $j = 2$ which is the case of E field parallel to the scattering plane. The curve in Fig. 4 with alternate long and short dashes gives $I_2^{CPOA}(\theta, ka = 500)$. It is evident that this CPOA describes the general rise in irradiance of the first coarse peak as θ decreases from 85 to 75 deg. The shift in the location of the peak near 65 deg is also well approximated by the model. This, and several other comparisons done for $j = 2$ with ka

from 100 to 1000 show that the CPOA does about as well in approximating the coarse structure for a coated bubble as the POA does for an uncoated bubble. See Fig. 6.

Now what about polarization $j = 1$ which is the case of E-field perpendicular to the scattering plane? It was evident from Fig. 5 (and other plots[10]) that the effect of the coating on the coarse structure is more than just an angular shift. The modulations of the coarse structure introduced by the coating may be attributed to the reflection of light at the coating water interface) as illustrated; e.g., by ray $(0,0)_b$ in Fig. 1. The scattering amplitude associated with this ray is larger for $j = 1$ than for $j = 2$ since for polarization $j = 2$ the local angle of incidence (i_b in Fig. 1) lies close to the Brewster angle of incidence $i_B = \tan^{-1}(n_c/n_w)$ for this interface. For a plane surface, the Fresnel reflection coefficient vanishes when $i_b = i_B$ for polarization $j = 2$ but for $j = 1$ there is no minimum in the reflection coefficient. Hence we understand why for $j = 1$ the coarse structure is disrupted by the coating so that scattering with $j = 1$ may be difficult to determine the bubble's radius.

Thus far we have discussed only the usual case of $n_c > n_w = 1.333$ where the specific examples in Fig. 4 and 5 had $n_c = 1.5$. Inspection of Eq. (4) leads to the prediction that $\Delta < 0$ in the unusual case of $n_c < n_w$. To confirm our general understanding of the effects of coatings, we computed the exact AKS for the case $j = 2$, $a = 37.5\ \mu m$, $h = 3.3\ \mu m$, and $n_c = 1.25$. Here the coarse peak was shifted to <u>smaller</u> θ (i.e., $\Delta < 0$ as predicted) and Eq. (5) well approximated the general rise in the coarse peak as θ decreased below 85 deg. It should be noted, however, that bubbles in the ocean would not have coating for which $n_c < n_w$.

C. Brewster-Angle Scattering from Coated and Uncoated Bubbles: Applications to Measurement of Film Thickness and to the Discrimination of Bubbles from Particles

The present section is concerned with properties of scattering of polarized light having the E-field parallel to the scattering plane ($j = 2$). Inspection of the Mie theory

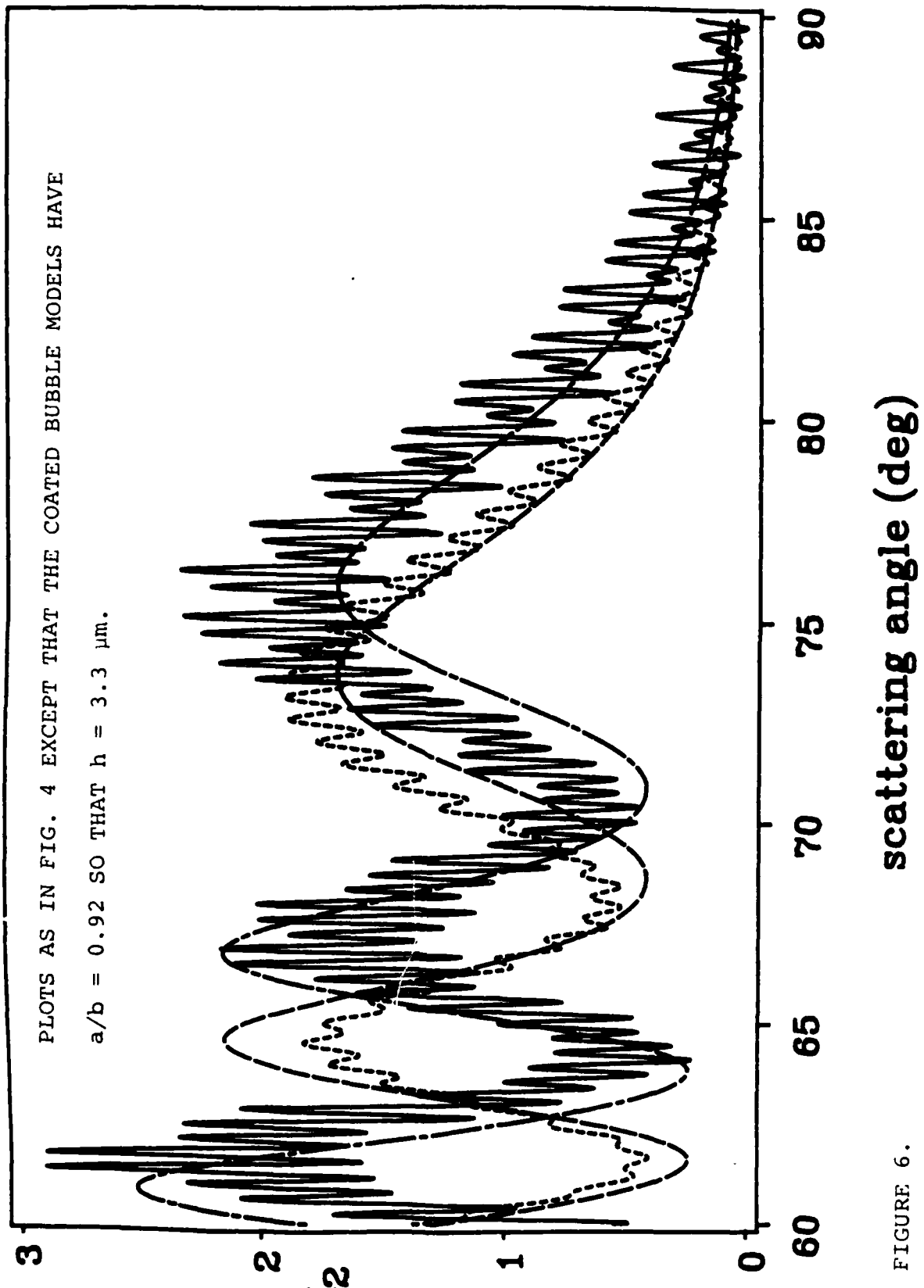
PLOTS AS IN FIG. 4 EXCEPT THAT THE COATED BUBBLE MODELS HAVE
a/b = 0.92 SO THAT h = 3.3 μm.
I_2
3
2
1
0
60
65
70
75
80
85
90
scattering angle (deg)

FIGURE 6.

results for the uncoated bubbles displayed as the solid curves in Fig. 3(a,b) reveals the following major features when the scattering angle $\theta \approx 106$ deg:

(a) Let $\langle I_2 \rangle$ denote a local angular average of the irradiance which masks the fine structure. This may be called the baseline irradiance. It is evident the $\langle I_2 \rangle$ is minimized for θ close to 106 deg.

(b) The visibility of the fine structure fringes in the vicinity of a given scattering angle θ may be denoted by

$$\text{Vis}(\theta) = \frac{I_{max} - I_{min}}{I_{max} + I_{min}}, \tag{6}$$

where I_{max} and I_{min} are local maximum and minimum values of I_2 closest to the specified θ. Inspection of the Mie results (solid curves in Fig. 3(a,b)) shows that $\text{Vis}(\theta)$ has a local minimum for θ close to 106 deg.

Consider the local angle of incidence i for the ray reflected from the water-air interface of the uncoated bubble. The aforementioned features are a consequence of i being close to the relevant Brewster angle $i_B = \tan^{-1}(n_w^{-1}) = \tan^{-1}(0.75) = 36.9$ deg. The scattering angle corresponding to $i = i_B$ is

$$\theta_B = 180 \text{ deg} - 2i_B = 106.2 \text{ deg}, \tag{7}$$

which may be called the Brewster scattering angle. Since the plane surface reflection coefficient has a null when $i = i_B$, it is to expected that $\langle I_2 \rangle$ is minimized for $\theta \approx \theta_B$ as was previously noted in Ref. 3 and 21.

Now the fine structure fringes in the angular region between θ of 82.8 deg and 120 deg are primarily a consequence of the interference between the far-side ray (the dashed (2,1) ray in Fig. 1) with the reflected ray (the dashed (0,0) ray). Since the amplitude of the reflected ray is minimized near $\theta \approx \theta_B$, so is the visibility, Eq. (6), of the interference pattern.

Figure 3 shows changes in the scattering near 106 deg which result from coating the bubble with a film having an index $n_c = 1.5$. These results are representative of other examples plotted in Ref. 10. The principal change is an increase of the baseline irradiance $\langle I_2 \rangle$ near 10o deg. This change is to be expected since the coating will mask the local null in the Fresnel reflection coefficient. Notice that $\langle I_2(106 \text{ deg}) \rangle$ is greater for the thicker of the two coatings (Fig. 3(b) as opposed to Fig. 3(a)). Results displayed in Ref. 10 suggest that $\langle I_2 (106 \text{ deg}) \rangle$ is a monotone increasing function of the film thickness h for a range of h; however, due to limited resources, this problem has not been examined in detail. It is plausible that the film thickness h could be determined from measurements of $\langle I_2 (106 \text{ deg}) \rangle$ or from the ratio ρ discussed below.

Another change evident in Fig. 3 caused by the coating is in the amplitude of the fine structure near 106 deg. These changes would certainly affect the visibility function, Eq. (6) near 106 deg though they might not be as useful for determining the film thickness.

There is an additional application of this Brewster-angle scattering which should be noted. Suppose bubbles in the ocean were not coated or that as in Fig. 3(a), the coating was so thin as to have only a minor effect on $\langle I_2 (106 \text{ deg}) \rangle$. Then it would be an easy matter to verify that the scatterer was in fact a bubble by measuring the ratio

$$\rho = \langle I_2(82.8 \text{ deg}) \rangle / \langle I_2(106 \text{ deg}) \rangle. \tag{8}$$

For such a clean bubble, ρ will be nearly independent of the radius a of the gas pocket if $a > 7$ μm. Computational results suggest that ρ will lie between 25 and 100. If the scatterer was a small spherical particle or biological cell having a refractive index $> n_w$, Mie theory typically gives $\rho < 1$. Hence such non-bubble scattering events could clearly be identified. Now for coated bubbles, it appears that ρ decreases and can have values as small as $\rho \approx 5$. Hence the identification of non-bubble events from the measured value of ρ may not be as easy. Nevertheless, it is recommended that the ratio ρ be measured for use along with the critical-angle scattering data.

D. Detector Placement and Inversion of Scattering Data to Obtain the Bubble Size on an Event-by-Event Basis

In addition to the task of computing and understanding the optical effects of surface films, the other major task of the contract was to consider how the light detectors should be placed so as to facilitate a measurement of a bubble's radius a. The geometry considered was intended to be realizable on instruments of the Wyatt Technology[22] design originally intended for studying the scattering from single marine microparticles in situ.[23] A region of water is considered to be illuminated by a Gaussian beam of polarized monochromatic light. For such a beam, the incident irradiance has the spatial dependence

$$i_{inc} = i_o \exp(-r^2/b^2), \tag{9}$$

where b is a parameter which specifies the effective beam radius and r is the distance from the axis of the beam. Bubbles drift through the scattering region and the light scattered by the bubbles is collected by a set of detectors; each having a well defined central scattering angle θ relative to the direction of the incident beam. The basic problem is to consider how to select the θ of a set of detectors.

As described in Sec. IIA-C of this report, the effects of a thin coating on the scattering pattern of a bubble are expected to be small if the incident light is polarized with the E-field parallel to the plane of the detectors. Consequently, we will limit our attention to such a configuration and model the scattering as if the bubble were not coated. In an experiment, the error introduced by a coating in the data inversion process could be estimated; however, it is presently anticipated that coating would not be the principal source of error when determining either the bubble radius or the absolute number density of bubbles.

Each detector produces a voltage proportional to the scattered irradiance averaged over the range of angles viewed. Denote this voltage by $v_j(\theta,t)$ where θ is the central scattering angle of that detector and the polarization index j has the value 2 for the

configuration considered. The v_j depend on time t because the bubble moves through the beam. The $v_j(\theta,t)$ are assumed to be recorded as a function of time. The principal problem with the use of a Gaussian beam, Eq. (9), is that the experimenter does not know how close the bubble comes to the axis of the beam. Let the minimum distance of the center of a bubble from this axis be denoted by y. Define an "event" as the passage of a single bubble through the beam; y may be thought of as an impact parameter relative to the beam's axis for a given event. If the radius a of the bubble is << b, the detected voltage will be maximized if $y = 0$ (such that the bubble is centered on the beam). Now for such an event, the detector at the critical angle $\theta = \theta_c = 82.8$ deg will produce a voltage v_2 which increases monotonically with the bubble radius a. It would then be a simple matter to invert the data on v_2 to obtain the radius for the bubble in each event. Unfortunately, when y is not known, inversion of the v_2 data is complicated.

Nevertheless, a procedure was formulated whereby the bubble radius for each event could be determined within a narrow range. It is assumed that $a << b$ and that the instantaneous scattering pattern could be well approximated by that for a plane wave with an incident irradiance given by Eq. (9) with r taken to be the instantaneous distance of the bubble from the beam axis. Some noteworthy features of this procedure are:

(a) Detectors are to be placed at the critical scattering angle, $\theta_c = 82.8$ deg and at several nearby angles having $\theta < \theta_c$.

(b) The voltages v_2 from these detectors will occur in ratios that are somewhat slowly varying functions of bubble radius a because the coarse structure (which occurs in the region $\theta < \theta_c$) varies slowly with a. Specifically, the ratios $v_2(\theta,t)/v_2(\theta = \theta_c,t)$ should be considered for that time t which maximizes $v_2(\theta_c,t)$ for a given event.

(c) It is anticipated that only a narrow range of radius values will give theoretical values for the aforementioned ratios consistent with data for scattering from

single bubbles. The mean value in this range, call it a_{exp} may be taken as the measured value for that event.

(d) The inversion procedure may be subjected to various statistical and internal consistency checks to test if it is operating properly. For example, from a_{exp} and the $v_2(\theta_c,t)$ data one could work backwards to determine the impact parameter y of each event. The resulting y should be randomly distributed in the viewed region. (Note, the viewed region of water may be limited by cutting off the irradiance so that i_{inc} drops to zero abruptly for large values of r.)

The details of this procedure were given.[14] Rather than repeat the description, the relevant portion of that report is reproduced as Appendix A to the present Final Report. Before proceeding, the reader is asked to examine Appendix A. Table II of the appendix lists recommended detector locations and angular widths.

Some comments on the method of event-by-event data inversion presented in Section A of Appendix A are appropriate.

(a) Figures A7-A10 of Appendix A were claimed to be plots of the normalized irradiances as a function of the bubble size parameter ka (see Table I for conversion to radius values) as given by the physical-optics approximation. Since those plots were prepared, a minor error in the POA computer algorithm used was corrected (see the Supplement Section of Ref. 10). The corrections are minor as may be seen by comparing the corrected POA curve, Fig. 7, with Fig. A8. These curves given the normalized scattering irradiance I_2 for θ = 75 deg. The corrections do not affect the applicability of the procedure. (Note: the original presentation and plots of the POA, Ref. 1-3 were free from the aforementioned computational error as are Fig. 4, 6, A2 of the present report.)

(b) Figures A7-A10 were intended to illustrate the method of data inversion. If this method is actually used for a real instrument, it would probably be

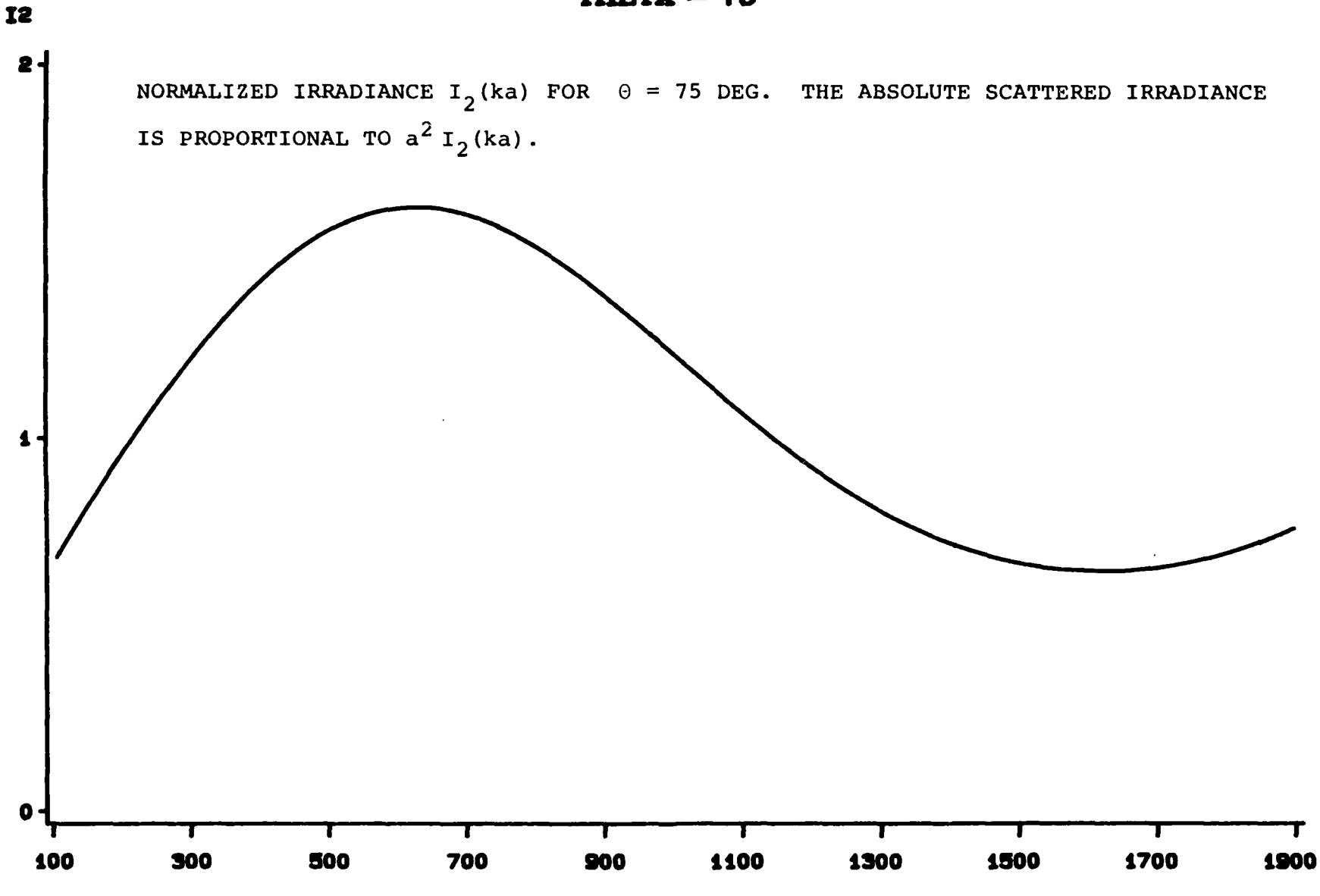

NORMALIZED IRRADIANCE $I_2(ka)$ FOR Θ = 75 DEG. THE ABSOLUTE SCATTERED IRRADIANCE IS PROPORTIONAL TO $a^2 I_2(ka)$.

FIGURE 7.

necessary to prepare plots (or tables) of the voltage ratios $v_2(\theta)/v_2(\theta = \theta_c)$ for the actual detector widths used by averaging the Mie theory results over the appropriate angular region for the range of bubble radii encountered in the experiments.

(c) To determine the absolute bubble concentration it is necessary to know the cross sectional area of the scattering region through which the water flows. The significance and control of this area is discussed in Sec. B.3 of Appendix A.

All of the aforementioned analyses assumes that there is only a single bubble in the scattering volume during the time t when $v_j(\theta_c,t)$ has its maximum value. It is also assumed there is no significant scattering of light bubbles in the volume of water which the beam passes through before it reaches the scattering volume. The problem of how to avoid or minimize the effects of multiple scattering was addressed[15] and the suggestions will not be repeated here. It is noteworthy that data which does not fit the predicted pattern for single bubbles, presented here in Appendix A and in Sec. C (for the Brewster scattering angle data), could be attributed either to scattering from more than one bubble or from particles and/or biological cells.

E. Statistical Properties of the Photodetector Voltages and a Possible Alternative to Event-by-Event Data Inversion

The maximum in the detector voltage output for a given bubble event will depend on how close the bubble came to the axis of the beam; this minimum distance is the impact parameter y discussed in the previous section. For a specific photodetector, the voltage output will pass through a maximum value as the bubble passes through the beam, see Fig. A1 of the Appendix. Let v denote this maximum value for a given event; v depends on the impacted parameter y of the event and for some value of y, v takes on a maximum value v_o which will depend on the radius a of the bubble. Assumptions will be noted

below concerning the statistics of y and the scattering of light from small bubbles in a Gaussian beam. These assumptions facilitate the prediction, below, of the statistical properties of the random variable $z = v/v_0$ for a sample of events in which all bubbles have the same radius. For the usual case in which bubbles in a sample of events are not all of the same size, that result could be used to predict the probability density function $\bar{F}(v)$ of the absolute voltages; it is also necessary, however, to know the size distribution (per radial interval) $n(a)$ of the polydisperse population of bubbles in the sample. It appears that in principle the problem may be turned around so that an unknown $n(a)$ might be found from the observed $\bar{F}(v)$; however, the details and stability of such an inversion process are yet to be examined.

The relevant statistical properties of $z = v/v_0$ for a monodisperse size distribution of bubbles will now be derived. It is assumed that the irradiance profile is described by Eq. (9) and that $a << b$ so that the scattered irradiance for a plane wave of irradiance given by the local value at the bubble's center;[24] these assumptions given

$$v(y) = v_0 \exp(-y^2/b^2), \tag{10}$$

where $v_0 = v(y = 0)$. Now the impact parameter y of each event is a random variable. It will be assumed that y is uniformly distributed between $y = 0$ and $y = y_{max}$ where for now we take $y_{max} \to \infty$. Let dN denote the number of events in interval between y and $y + dy$. The uniform distribution of impact parameters gives

$$\frac{dN}{dy} = D, \tag{11}$$

where D is a constant (i.e., D does not depend on y).

The random variable $z = v/v_0$ is related to y by Eq. (10). The desired quantity is the probability density function $F(z)$. For a sample of events having a large number of bubbles of the same size, the frequency of occurrence of event voltages between v and $v + dv$ will be proportional to $F(v/v_0)v_0^{-1}dv$. The expression

$$F(z) = v_o|dN/dv| = (dN/dy)|dy/dz|, \tag{12}$$

may be shown to be consistent with rules governing the statistics of transformed random variables. Now Eq. (10) gives

$$dz/dy = -2yb^{-2}z = -2b^{-1}\, z[-\ln(z)], \tag{13}$$

where $0 \le z \le 1$. Equations (11) - (13) yield

$$F(z \le 1) = A[z(-\ln z)^{1/2}]^{-1} \tag{14a}$$

$$F(z > 1) = 0 \tag{14b}$$

where the constant $A = Db/2$.

The density function F in Eq. (14) diverges as $z \to 0$ because the Gaussian beam was assumed to be unbounded and upper bound y_{max} for the impact parameters was also taken to be infinite. For a beam in which the irradiance is cut off at some finite distance from the axis, this divergence in $F(z)$ is removed. As $z \to 1$, $F(z)$ diverges because of the flatness of the irradiance profile in the center of the beam. Except for these divergences F in Eq. (14) is smooth and F takes on a minimum value at some intermediate z. The divergence of F as $z \to 1$ is desirable as noted below.

Let $\bar{F}(v)$ denote the probability density function of the absolute voltage v for a sample consisting of many events in which the bubbles were not all of the same size. The frequency of occurrence of event voltages between v and $v + dv$ will be proportional to $\bar{F}(v)\, dv$. Let $n(a)$ denote the number of bubbles having radii between a and $a + da$; $n(a)$ is the size distribution for the sample. The statistical properties of the v are governed by

$$\bar{F}(v) = \bar{N}^{-1} \int_0^\infty n(a)\, F(v/v_o)da, \tag{15}$$

where $\bar{N}$ is the total number of bubbles in the sample; v_o depends on the bubble radius a through the scattering law appropriate for the detector considered. It is desirable that v_o be a monotonic increasing function of a; this may be achieved by letting the detector be centered on the critical scattering angle $\theta = 82.8$ deg and by polarizing the incident beam so that the E-field lies in the scattering plane (i.e., j = 2). For example, the Physical Optics Approximation[1,2,5] yields the following proportionality

$$v_o = Ga^2 \tag{16}$$

where G is a constant which depends on the light power and the detector sensitivity.[25] Notice that divergence in F(z) as $z \to 1$ is desirable since this causes $\bar{F}(v)$ to retain information concerning the size distribution n(a). Furthermore, it would be desirable to remove the divergence in F(z) as $z \to 0$ by cutting off the beam at some finite distance from the axis. Of course, for a finite beam with a flat irradiance profile $F(z) \propto \delta(z-1)$ where δ is the Dirac δ function; in that case the inversion to give n(a) from data for $\bar{F}(v)$, by way of Eqs. (15) and (16), would be easy.

IV. STUDENTS WHO WORKED ON THIS CONTRACT

1. Stuart C. Billette
2. Cleon E. Dean

V. REFERENCES

1. P. L. Marston and D. L. Kingsbury, "Scattering by a Bubble in Water Near the Critical Angle: Interference Effects," J. Opt. Soc. Am. 71, 192-196 (1981); 71, 917 (1981).
2. D. L. Kingsbury and P. L. Marston, "Mie Scattering Near the Critical Angle of Bubbles in Water," J. Opt. Soc. Am. 71, 358-361 (1981).

3. P. L. Marston, D. S. Langley, and D. L. Kingsbury, "Light Scattering by Bubbles in Liquids: Mie Theory, Physical-Optics Approximations, and Experiments," Applied Scientific Research 38, 373-384 (1982).

4. P. L. Marston, D. S. Langley, and D. L. Kingsbury, Technical Report No. 1, Light Scattering by Bubbles in Liquids or in Glass, issued September 1981 for O.N.R. Contract N00014-80-C-0838 (available from the Defense Technical Information Center, Cameron Station, Alexandria, VA, Accession No. AD-A104241) 90 pages.

5. D. S. Langley and P. L. Marston, "Critical-Angle Scattering of Laser Light from Bubbles in Water: Measurements, Models, and Applications to Sizing of Bubbles," Applied Optics 23, 1044-1054 (1984).

6. P. L. Marston, Research on Acoustical Scattering, Optics of Bubbles, Diffraction Catastrophes, and Laser Generation of Sound by Bubbles, Report No. N00014-85-C-0141-AR5, issued September 1985 (available from the Defense Technical Information Center, Cameron Station, Alexandria, VA, Accession No. AD-A161333) 72 pages.

7. P. L. Marston, Research on Acoustical Scattering, Diffraction Catstrophes, Optics of Bubbles, Photoacoustics, and Acoustical Phase Conjugation, Report No. N00014-85-C-0141-AR6, issued October 1986 (available from the Defense Technical Information Center, Cameron Station, Alexandria, VA, Accession No. AD-A XXXXXX) 48 pages.

8. P. L. Marston, J. L. Johnson, S. P. Love, and B. L. Brim, "Critical Angle Scattering of White Light from a Cylindrical Bubble in Glass: Photographs of Colors and Computations," Journal of the Optical Society of America 73, 1658-1664 + Plate X (1983).

9. P. L. Marston, Critical Angle Scattering by a Bubble: Physical-Optics Approximation and Observations," J. Opt. Soc. Am. 69, 1205-1211 (1979); 70, 353 (1980).

10. S. C. Billette and P. L. Marston, "Computational Analysis of the Effects of Surface Films on the Optical Scattering Properties of Bubbles in Water," Technical Report issued under contracts N00014-86-K-0242 and N00014-85-C-0141 (October, 1986), Accession Number AD-AXXXXXX (Defense Technical Information Center, Alexandria, VA) 166 pages.

11. S. C. Billette and P. L. Marston, "Scattering of light by a coated bubble in water near the critical scattering angle" (abstract only), to appear in J. Opt. Soc. Am. 13 (1986). Presented at the Annual Meeting of the Optical Society of America (Seattle, WA, October 1986).

12. P. L. Marston and S. C. Billette, "Scattering of light by a coated bubble in water near the critical and Brewster scattering angles" (abstract only), J. Acoust. Soc. Am. Suppl. 80, 59 (1986).

13. P. L. Marston, "Progress Report on Research Supported by Contract N00014-86-K-0242, Part 2: The Effects of Surface Films on Some Optical Scattering Properties of Bubbles in Water" (July 2, 1986).

14. P. L. Marston, "Progress Report on Research Supported by Contract N00014-86-K-0242, Part 1: Detector Placement and Inversion of Light Scattering Data for the Bubble Size Spectrometer of the Wyatt Technology Design" (May 29, 1986).

15. Informal progress letter by P. L. Marston to M. Y. Su (dated April 25, 1986).

16. Letter by P. L. Marston to M. Y. Su (dated June 17, 1986) on the generation of microbubbles for calibration purposes.

17. B. D. Johnson and R. C. Cooke, "Generation of Stabilized Microbubbles in Seawater," Science 213, 209-211 (1981).

18. V. V. Goncharov et al., "Determination of the diffusion constant of a gas bubble in sea water from the solution of air bubbles in the medium," Soviet Physics Acoustics 30, 273-275 (1984).

19. R. E. Glazman, "Effects of adsorbed films on gas bubble radial oscillations," J. Acoust. Soc. Am. 74, 980-986 (1983).

20. A. L. Aden and M. Kerker, "Scattering of electromagnetic waves from two concentric spheres," J. Appl. Phys. 22, 1242-1246 (1951).

21. D. L. Kingsbury and P. L. Marston, "Scattering by Bubbles in Glass: Mie Theory and Physical Optics Approximation," Applied Optics 20, 2348-2350 (1981).

22. Wyatt Technology, 820 East Haley St., Santa Barbara, CA 93103-3003.

23. P. J. Wyatt, "A new instrument for the in-situ measurement of individual marine particulates: Laser Troller," in Ocean Optics VIII, Proc. SPIE 637 (at press); P. J. Wyatt and S. D. Phillips, "Laser Trolling for Microparticles," Proceedings of the 1985 Scientific Conference on Obscuration and Aerosol Research, edited by R. H. Kohl (U. S. Army, Aberdeen Proving Ground, MD, 1986) pp. 209-220.

24. If the bubble radius a is not << the beam parameter b, the maximum voltage v should occur when the bubble's center is displaced slightly from the axis of the beam. This displacement may be neglected, however, when $a << b$ so that it becomes a good approximation to take the maximum v at $y = 0$.

25. Even if the detector is displaced slightly from the critical scattering angle, the voltage v_0 can be a monotone increasing function of bubble radius a over a wide range of a. This was illustrated for $\theta = 80$ deg in G. M. Hansen, "Mie scattering as a technique for the sizing of air bubbles," Applied Optics 24, 3214-3220 (1985).

VI. APPENDIX A: DETAILS OF INVERSION PROCEDURE (REPRODUCED FROM REF. 14)

A. Detector Placement and Proposed Inversion Procedure Based on Relative Scattered Irradiances

1. Introduction--

In item 4(f) of my letter of April 25 I indicated that other detectors would be needed at angles more forward than $\theta_c = 82.8$ deg. I now explain the positioning and use of such detectors. Let $v_j(\theta,t)$ denote the voltage output of a given detector multiplied by a sensitivity factor determined during calibration: $j = 2$ for a detector in the plane parallel to the incident wave's E polarization; $j = 1$ for a detector in the plane perpendicular to the incident wave's E polarization; θ denotes the central scattering angle viewed by the detector. For a perfectly isotropic and unpolarized point source located in the center of the scattering volume, the v_j for all θ should have the same value.

Suppose now the $v_j(\theta,t)$ are in response to a bubble which drifts through the scattering volume. As a function of time t the signal for an "event" might look something like that shown in Fig. 1:

Fig. A1

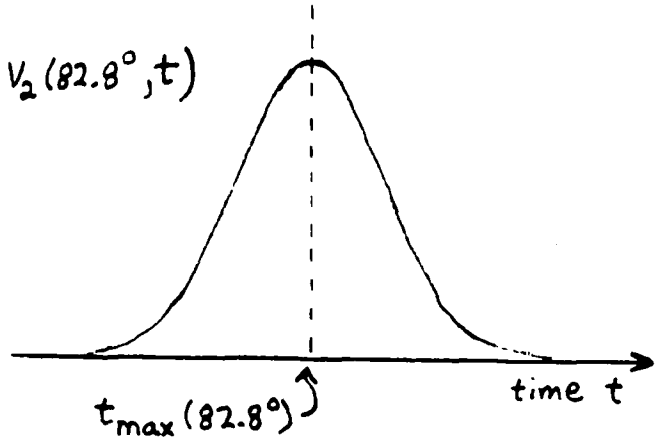

where I have chosen to take $\theta = 82.8°$ and $j = 2$ since that is a particularly convenient reference for reasons noted below. The Gaussian shape of curve reflects the assumption that the bubble moves at a fixed velocity through a Gaussian beam; however, neither assumption is essential to the analysis which follows. Let

$v_j(\theta,t_{max}\,(82.8°)) \equiv v_j(\theta)$ such that, for now, I only use data from all the detectors for the time interval in which $v_2(82.8°,t)$ is maximized, that is, at $t = t_{max}\,(82.8°)$. (Note it is to be anticipated that for spheres the other $v_j(\theta,t)$ would be maximized at the same t if the bubble radius a << the beam width.) Unfortunately, the values of $v_2\,(82.8°) \equiv v_2\,(82.8, t_{max}\,(82.8°))$ do not by themselves give the bubble radius on a event-by-event basis since the impact parameter y of a bubble, relative to the center of the beam, is not known. Nevertheless, I show in Section B that the absolute magnitude of $v_2\,(82.8°)$ for each event is useful both for augmenting and for checking the data inversion procedure given below.

The problem now reduces to finding the bubble radius a for a given event from the relative outputs

$$W_j(\theta) \equiv v_j(\theta)/v_2(82.8°) \qquad (1)$$

for a small set of detectors at various θ. The procedure listed below is based on ideas which I presented at NORDA in January 1985.

2. Review of Scattering Theory Results--

Figures 2-5 show the computed normalized irradiances I_2 for j = 2 (E field parallel to the plane of scattering). The normalization is my usual one in which the geometric (isotropic) reflection from a perfectly reflecting sphere of the same radius gives $I_j = 1$. Except as noted below the solid curves are from Mie theory, which is the exact result for an uncoated sphere while the dashed curves are from the Marston-Kingsbury Physical Optics Approximation (JOSA, 1981). Figure 4 also shows results for a thinly coated bubble (the solid curve in this case) where the Mie theory (for an uncoated bubble) is the curve with short dashes. The fine structure is larger in amplitude for the coated sphere than for the uncoated sphere but in both cases the coarse structure is well approximated by the POA. Figure 6

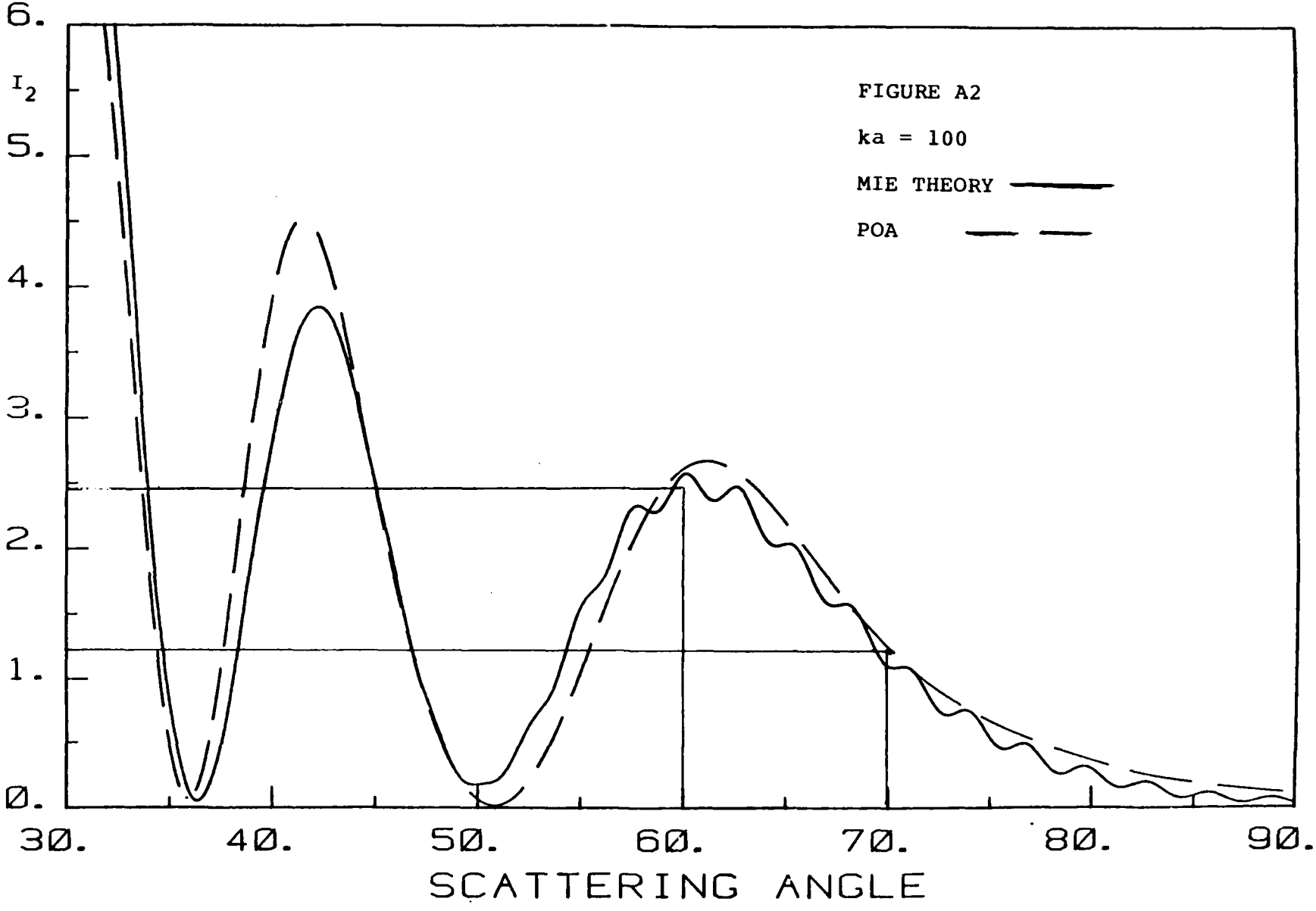
6.
I_2
5.
4.
3.
2.
1.
0.
30.
40.
50.
60.
70.
80.
90.
SCATTERING ANGLE
FIGURE A2
ka = 100
MIE THEORY
POA

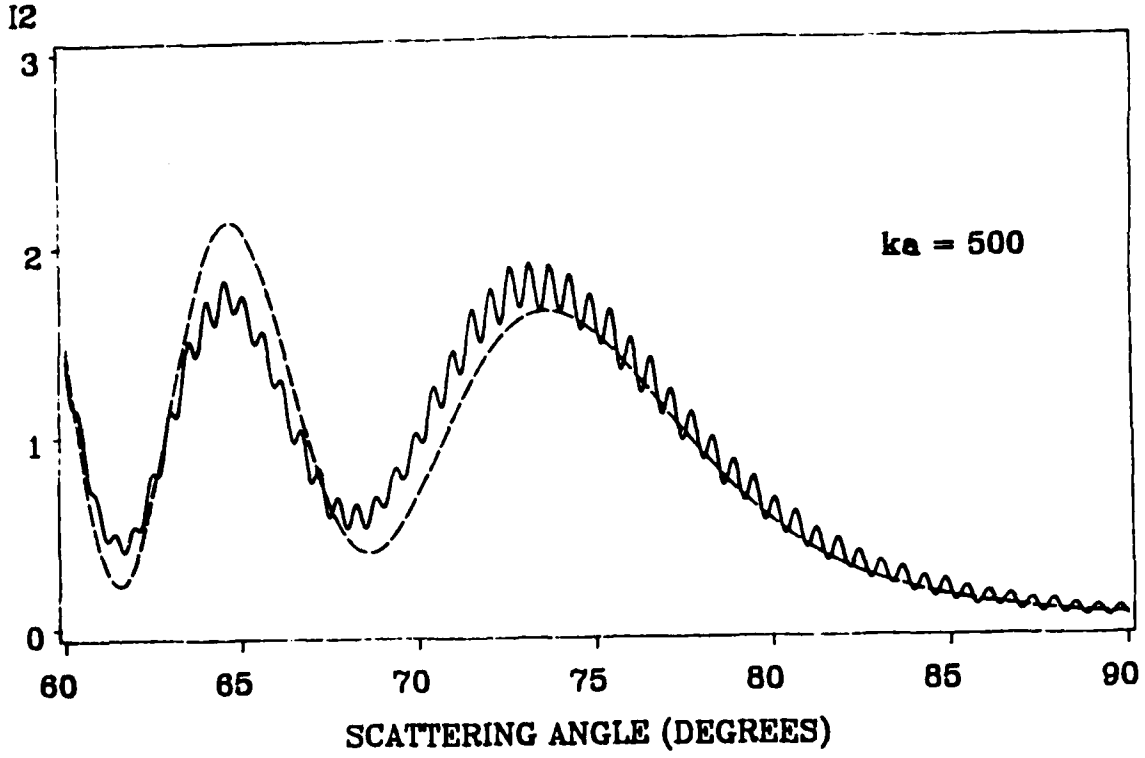
I2
3
2
1
0
ka = 500
60
65
70
75
80
85
90
SCATTERING ANGLE (DEGREES)

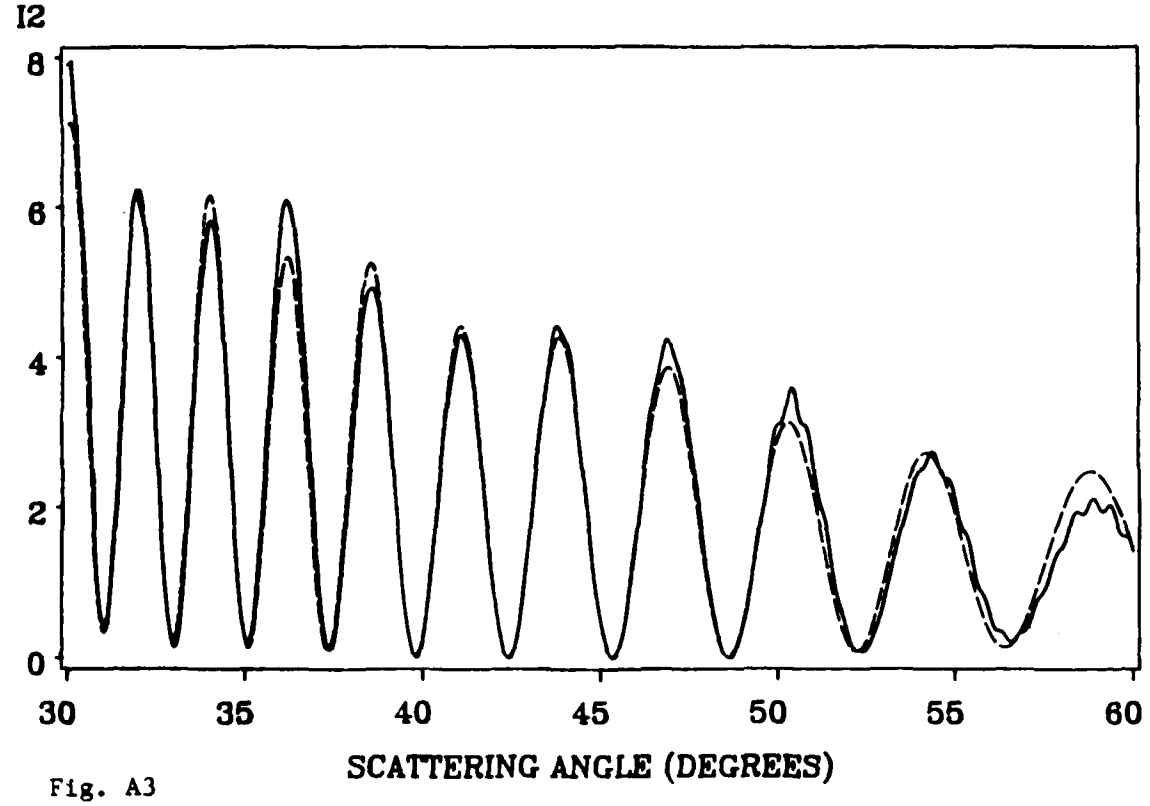
I2
8
6
4
2
0
30
35
40
45
50
55
60
SCATTERING ANGLE (DEGREES)

Fig. A3

KA = 1000

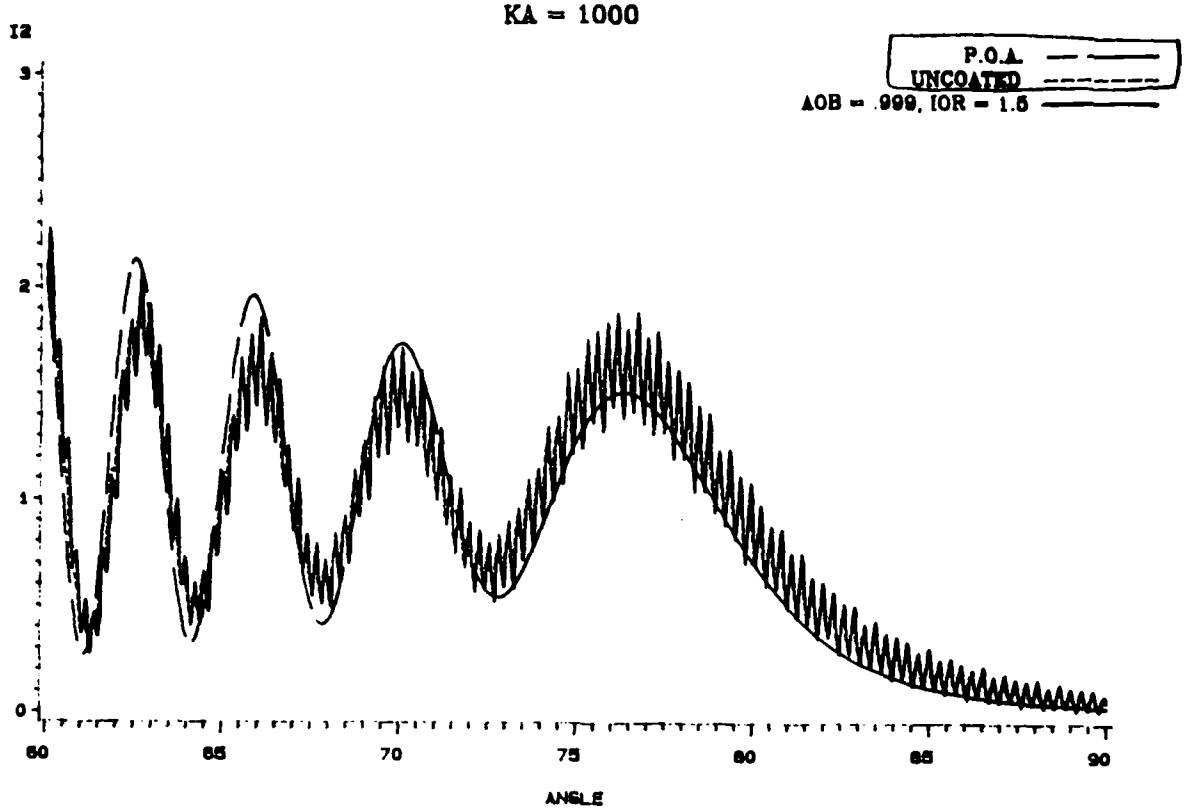

KA = 1000

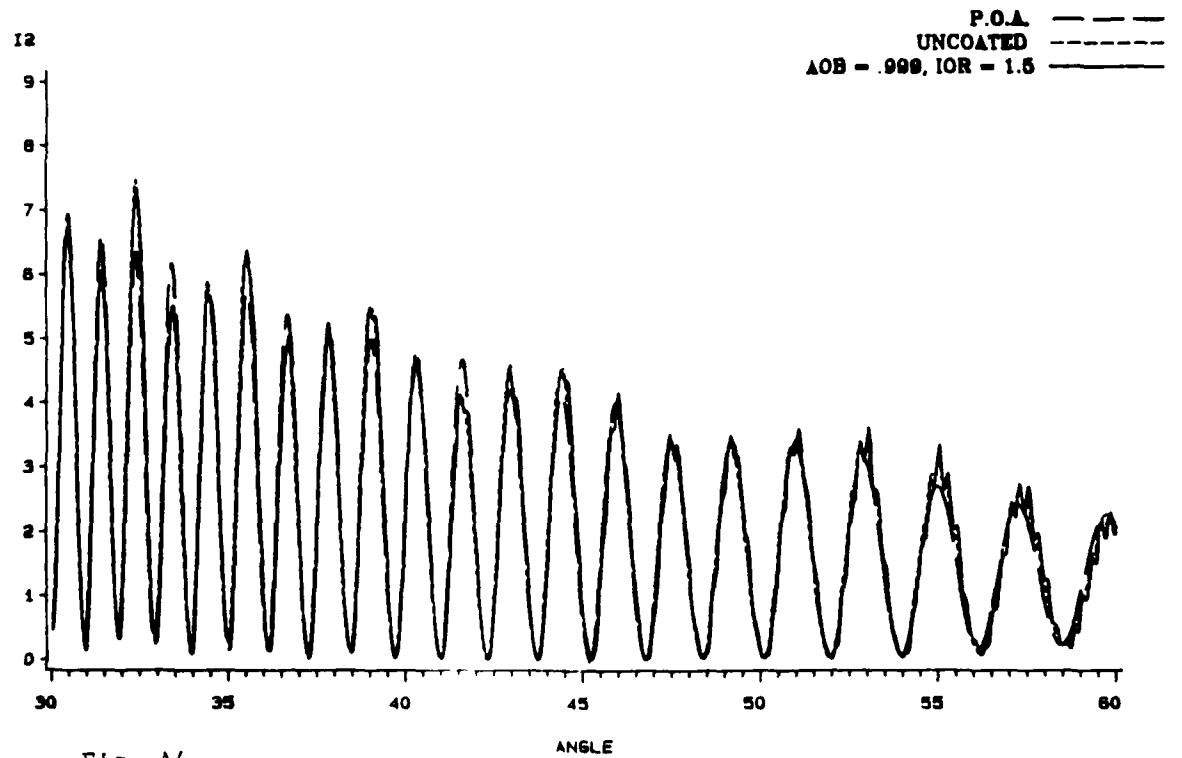

Fig. A4

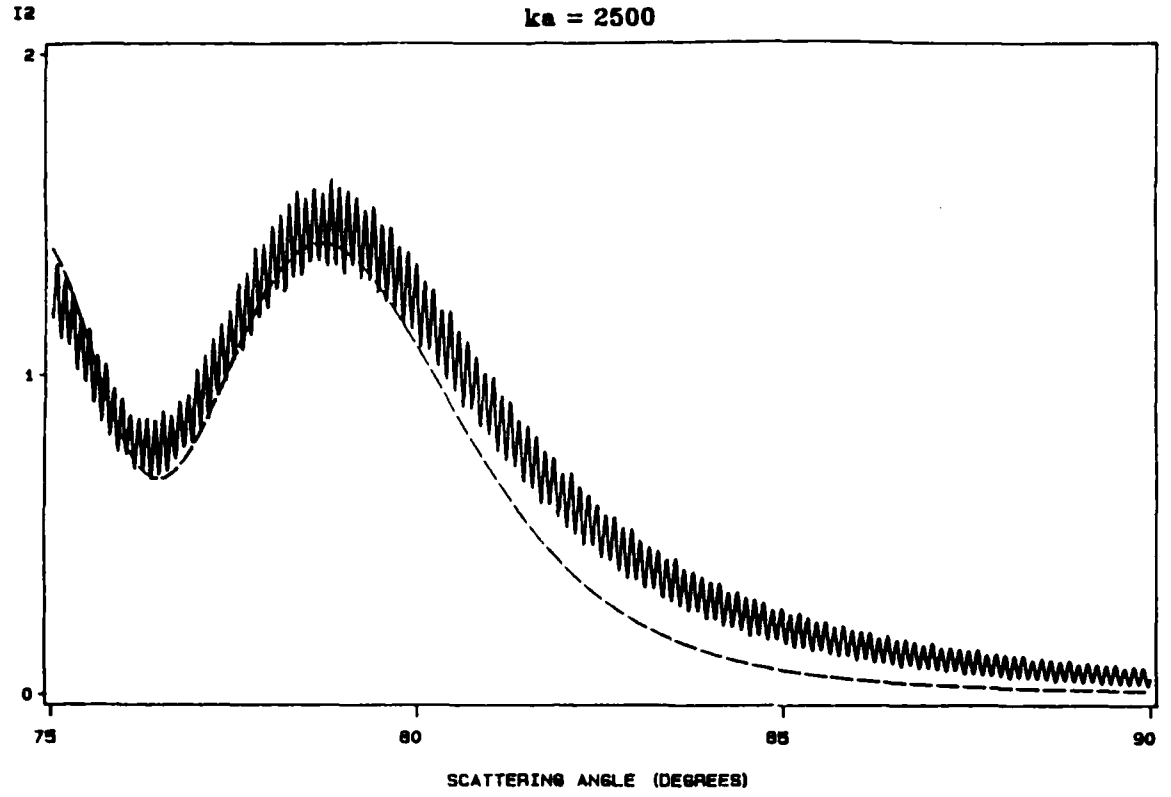
I2
ka = 2500
2
1
0
75
80
85
90
SCATTERING ANGLE (DEGREES)

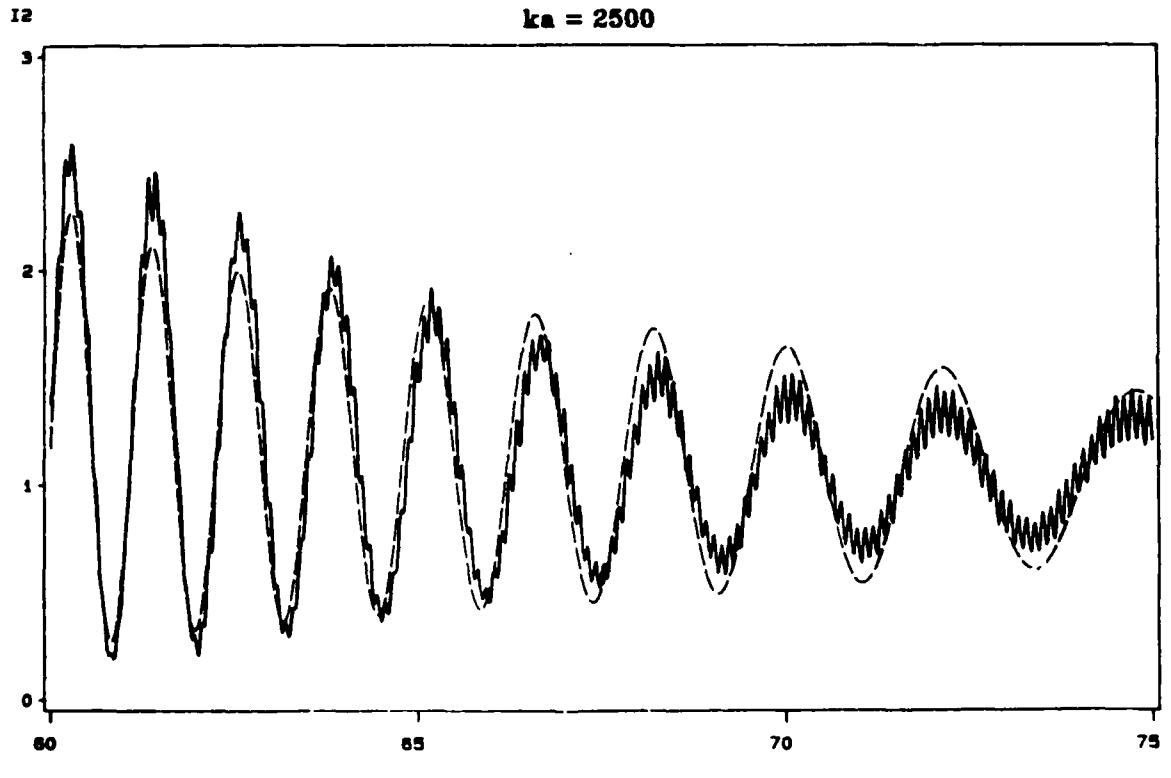
I2
ka = 2500
3
2
1
0
60
65
70
75
SCATTERING ANGLE (DEGREES)

Fig. A5

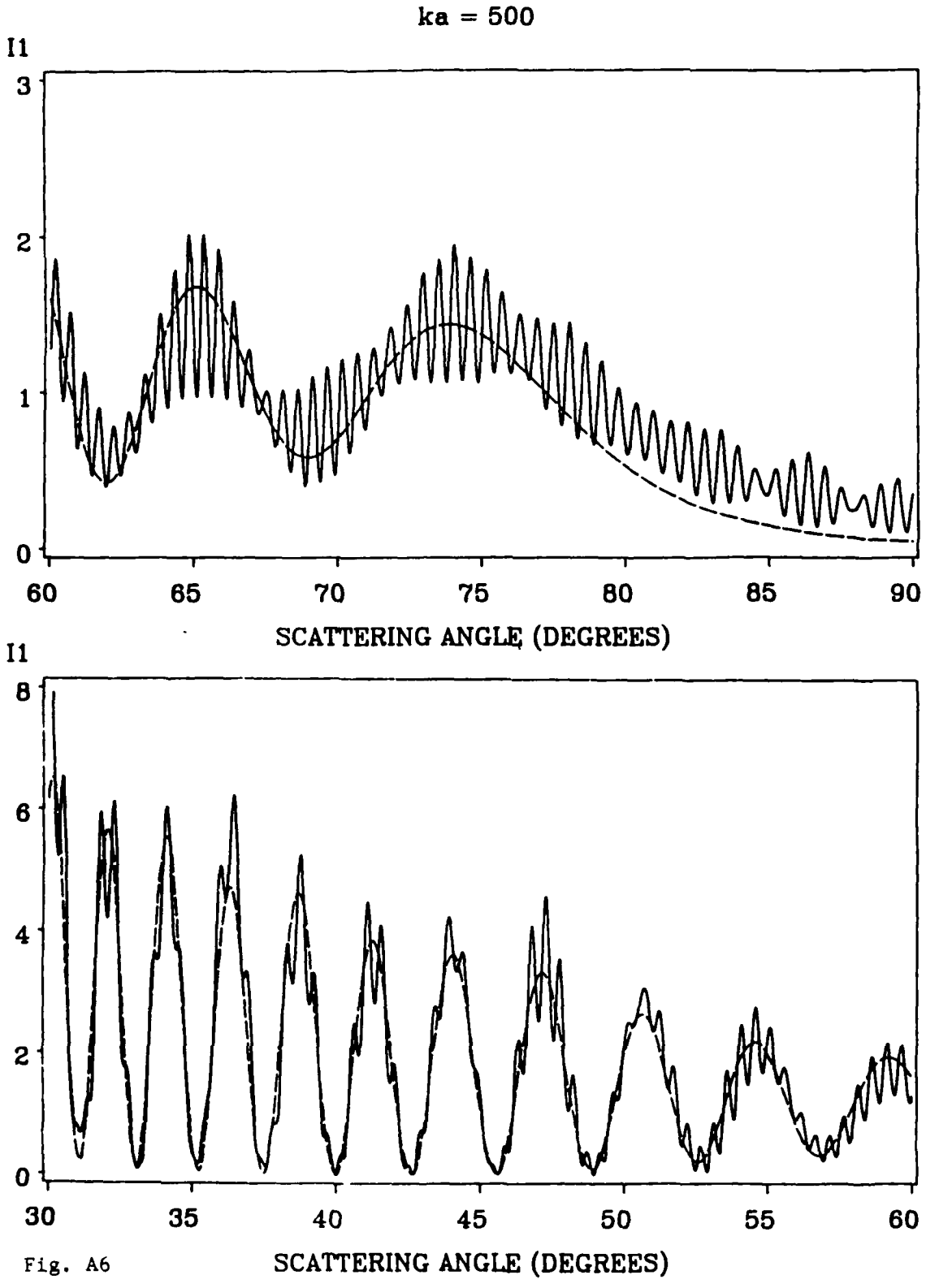
ka = 500
I1
3
2
1
0
60
65
70
75
80
85
90
SCATTERING ANGLE (DEGREES)
I1
8
6
4
2
0
30
35
40
45
50
55
60
SCATTERING ANGLE (DEGREES)

Fig. A6

shows the $j = 1$ (E perpendicular to scattering plane) case for $ka = 500$ and is to be compared with Fig. 3 for the corresponding $j = 2$ case. It is seen (as noted in my various previous publications) that: (i) the fine structure is much smaller in magnitude for $j = 2$ than for $j = 1$; (ii) the Mie results averaged near $\theta_c = 82.8°$ are closer to the universal POA value of $I_j(\theta_c) = 1/4$ for the case $j = 2$ than for $j = 1$; (iii) for both $j = 1$ and $j = 2$ the underlying coarse structure is well approximated by the POA, and (iv) both the Mie theory and the POA show only small differences in the locations of the coarse peaks between the cases $j = 1$ and $j = 2$ so that it is unlikely that these differences would be useful measuring ka.

For light from a He-Ne laser $\lambda_{air} = 633$ nm, $\lambda_{water} = (3/4)\,\lambda_{air}$, and $k = 2\pi/\lambda_{water}$. The relation between the ka and the bubble radius a and diameter 2a is listed below in Table I.

Table I

ka	radius = a (μm)	diameter = 2a (μm)
100	7.5	15
500	38	76
1000	75	150
2500	189	378

3. Difficulties Measuring the Size of Objects from Limited and Relative Scattering Data at Large ka--

Inspection of Figs. 2-6 show that near θ_c the coarse structure is one or more order(s) of magnitude broader than the fine structure. The fine structure spacing $\Delta\theta_{fine}$ at 82.8° is approximately (Langley, Marston, Applied Optics 1984) for this wavelength:

$$\Delta\theta_{fine} \text{ (degrees)} \approx (1/45)\,(a \text{ mm})^{-1}, \qquad (2)$$

Also our Mie calculation near forward scattering show the spacing of the forward diffraction peak is of the same magnitude as $\Delta\theta_{fine}$ given by this approximation. Hence because of the large size of the bubbles to be studied and because very closely spaced detectors are not feasible with the Wyatt instrument, there is no point in trying to use either the fine structure or the spacing of the forward diffraction peaks to measure the sizes. At best, we can hope to minimize the complications due to fine structure by taking $j = 2$ and, for each detector, by averaging over a small range of scattering angles (see item 6 of letter of April 25). The point is that even if the detectors could easily resolve the fine structure, for the purpose inverting scattering data it would be impossible to say which fine fringe was being viewed! This is because physical considerations limit the spacing between detectors to about 5° which is $>> \Delta\theta_{fine}$.

4. Inversion Procedure Based on Coarse Structure--

For the reasons noted above it is fortunate that the coarse structure exists and that it has a well defined starting angle, $\theta_c = 82.8$ deg. As outlined below it should be possible with a few detectors placed close to θ_c to measure a for the size range of interest roughly ka = 100 - 2500, and if necessary down to ka ≈ 25.

Figure 7 shows the normalized irradiance I_2 ($\theta = 70$ deg) plotted as a function of ka. The plot is given by the POA and hence does not include any fine structure. Since a perfectly reflecting sphere has an irradiance proportional to a^2 the actual irradiance and detector output is proportional to a^2 times the function plotted in Fig. 7. According to the physical optics approximation I_j (82.8 deg) = 0.25 so that the ratio of the detector outputs becomes:

$$W_j(\theta) \equiv v_j(\theta)/v_2(82.8 \text{ deg}) \approx 4\, I_j(\theta). \qquad (3)$$

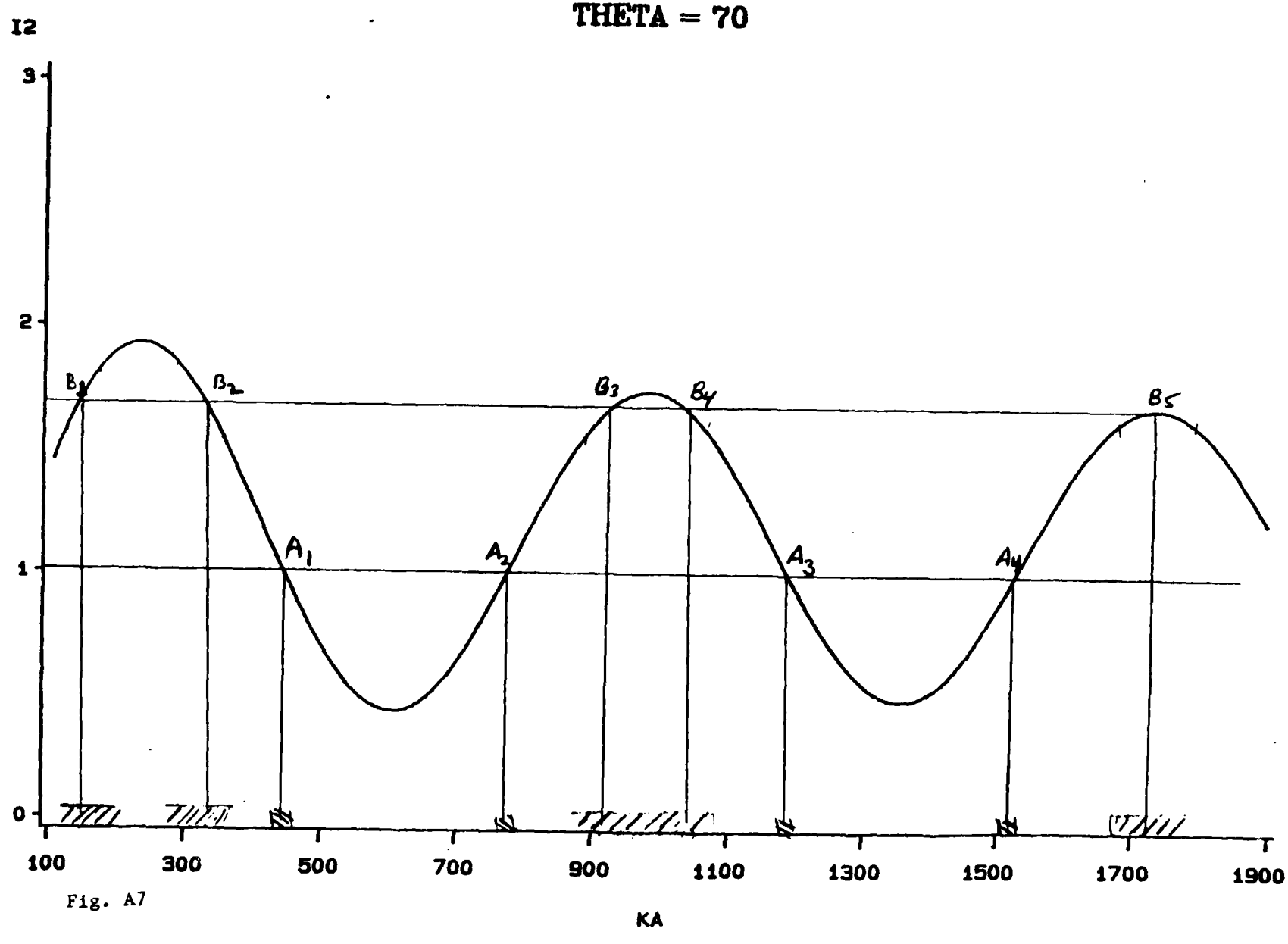
THETA = 70
I2
3
2
1
0
B1
B2
B3
B4
B5
A1
A2
A3
A4
100
300
500
700
900
1100
1300
1500
1700
1900
KA

Fig. A7

Suppose v_2 (70 deg) and v_2 (82.8 deg) are measured for a given event such that W_2 (70 deg) = 4.0 so that Eq. (3) gives I_2 (70 deg) = 1.0. Then, except for the unusual case of bubbles outside the range ka = 100 - 2000, we would expect the ka for this bubble to be given by one of the roots labeled A_1, A_2, A_3, and A_4 of the condition I_2 (70 deg) = 1.0. Ideally, to determine which root we could use the absolute magnitude of v_2 (82.8 deg); however, since we do not know the bubbles impact parameter relative to the center of the Gaussian beam v_2 (82.8 deg) is of limited use (see Sec. B of this report). To discriminate which A_n is appropriate for this event we may use the $v_j(\theta)$ for other detectors and apply Eq. (3).

With this task in mind, Figs. 8-10 show $I_2(\theta)$ for θ = 75, 65, 60, and 50 deg * according to the POA. It is evident that v_2 (75 deg), and hence I_2 (75 deg), would be especially useful in this task except when the experimental I_2 (75 deg) lies close to one of extremum of Fig. 8. Thus the roots A_3 and A_4 may be clearly distinguished from A_1 and A_2 by using the measured value of I_2. By using a measured value, via Eq. (3), of either I_2 (65 deg) or I_2 (60 deg) one can say with certainty which of A_1 or A_2 is appropriate.

One complication of this procedure is for the case where the measured I_2 (70 deg) lies close to one of the extremum of Fig. 7. This is the case shown with roots B_1 - B_5. Because of uncertainties in both the measurement and the theory, a wide range of ka roots are now possible as indicated by the dark band on the ka axis below roots B_3 and B_4 in Fig. 7. Figure 8 suggests that I_2 (75 deg) may be useful for distinguishing between various roots. Inspection of Figs. 10 and 11* show that neither measurement of I_2 (60 deg) nor measurement of I_2 (50 deg) would be of any use in discriminating between roots B_3 and B_4. This is because the band of pos- sible values for ka spans one or more cycles of the coarse structure present in I_2 (when plotted as a function of ka). The ka spacing between these oscillations decreases as θ is reduced. There is a corresponding decrease in the angular spacing at fixed ka in

*Fig.11 for 50 deg is omitted from this APPENDIX. It is like Fig. 10 except the coarse structure is even more closely spaed in ka.

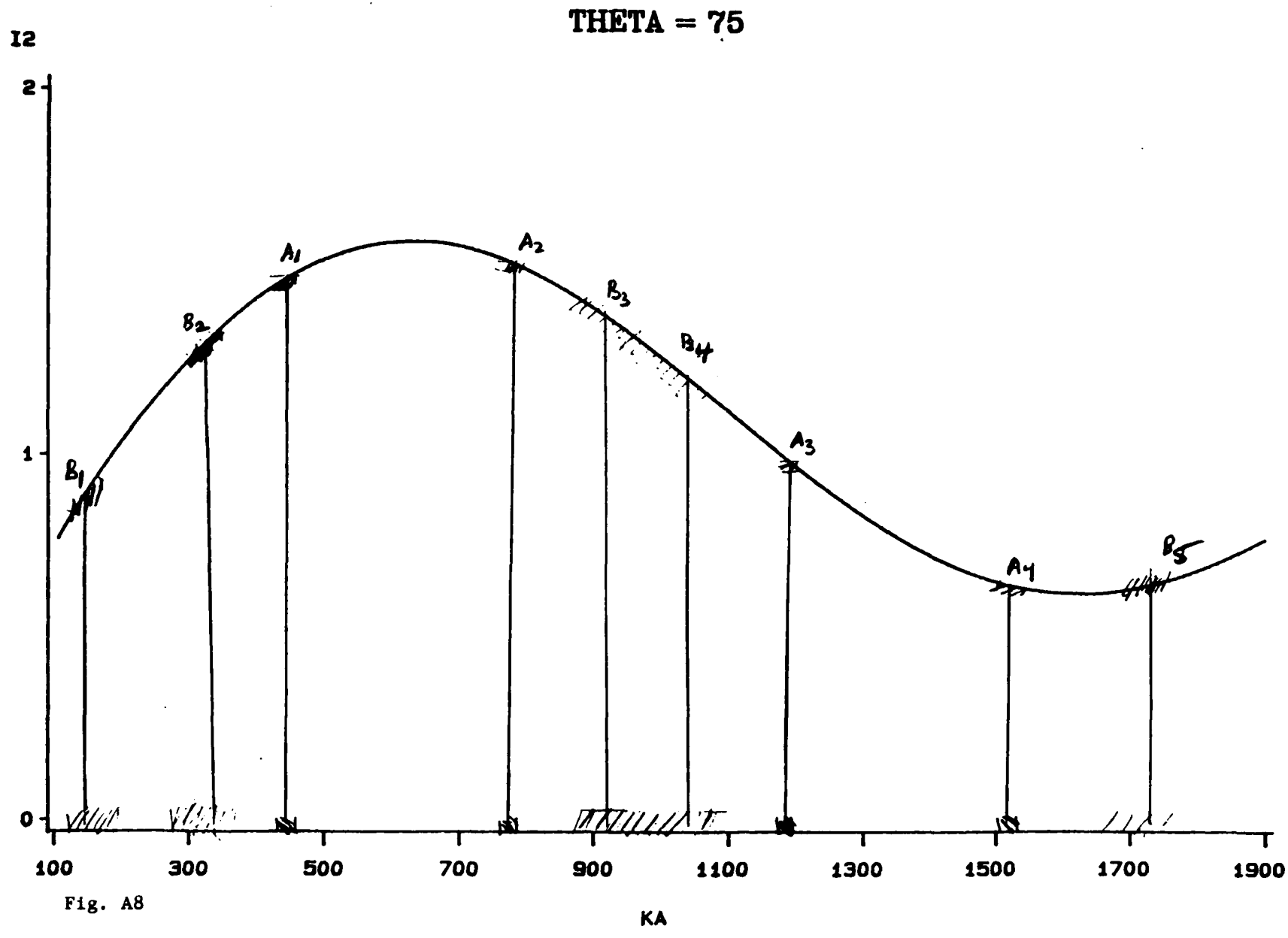
THETA = 75
I2
2
1
0
A1
A2
A3
A4
B1
B2
B3
B4
B5
100
300
500
700
900
1100
1300
1500
1700
1900
KA

Fig. A8

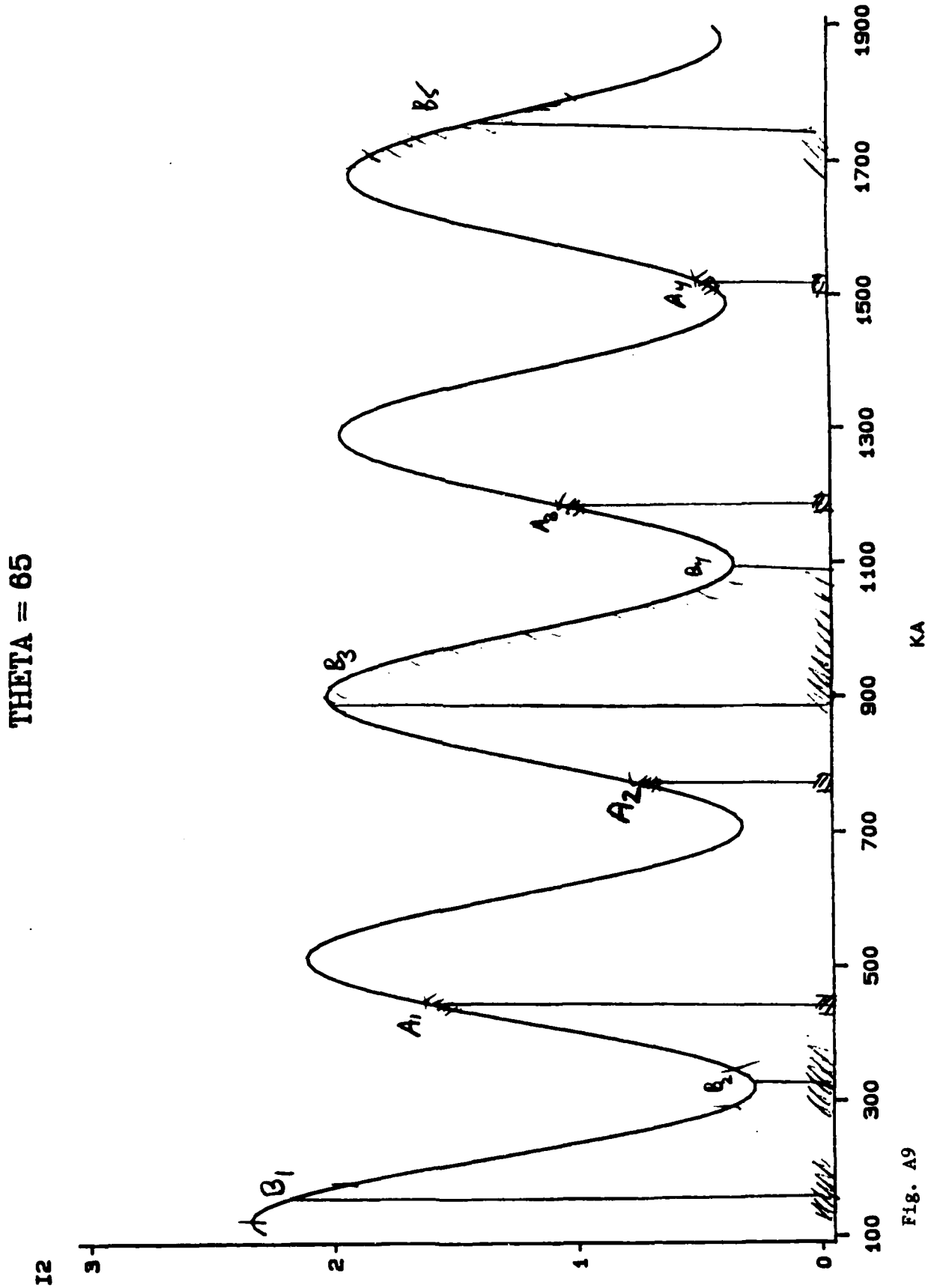
THETA = 85
I2
3
2
1
0
100
300
500
700
900
1100
1300
1500
1700
1900
KA
B1
A1
B2
A2
B3
A3
B4
A4
B5

Fig. A9

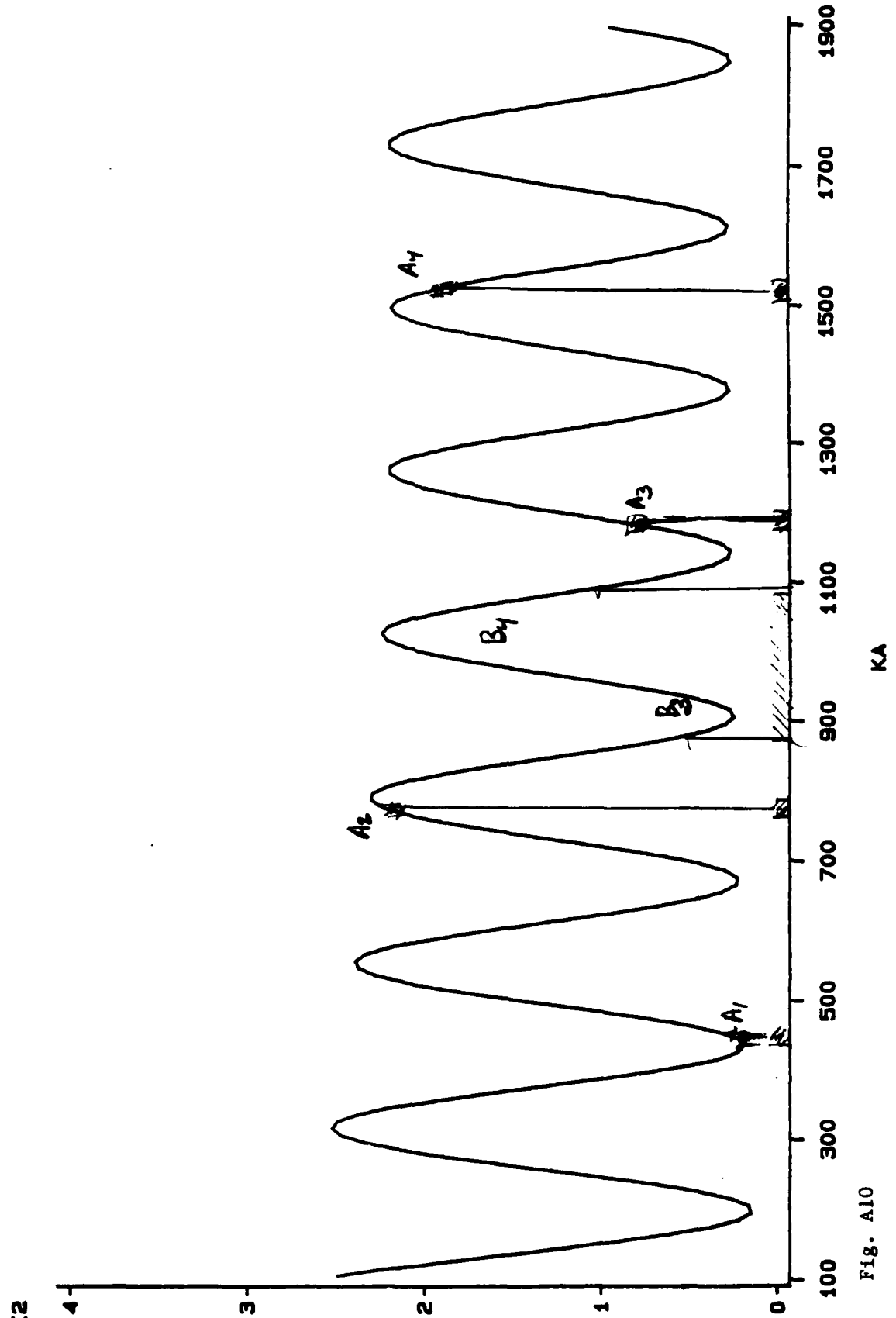
THETA = 60
I2
KA
A1
A2
A3
A4
B2
B4
0
1
2
3
4
100
300
500
700
900
1100
1300
1500
1700
1900

Fig. A10

the coarse structure as θ decreases. See Figs. 3-6. It is dif- ficult to use measurements of $v_j(\theta)$ (and hence $I_j(\theta)$) for $\theta \leq 60$ deg since it will be difficult to say with certainty which of the coarse oscillations is being viewed. (Recall that the situation for using the fine structure with discretely spaced angular detectors is even more hopeless.) Hence to make optimum use of the coarse struc- ture I recommend that as many detectors as possible be spaced between $\theta = 65$ deg and $\theta = 82.8$ deg. To reduce the complications of averaging over the fine fine structure, these should be placed on the great circle which is contained in the plane of the E polarization of the incident wave. This corresponds to $j = 2$ scattering. This inversion procedure may be augmented with proper use of the absolute amplitude. See Section B2 of this report.

5. Summary of Recommendations on Detector Placement --

In addition to the detectors placed as noted in item 4(a)-(d) of my letter of April 25, I recommend that as many as possible of the following detectors be placed in the $j = 2$ great circle. These are listed in roughly the order of priority.

Table II. Recommended Detectors

I.D. No.	Scattering angle at the center of the detector (deg)	Full angular width viewed by the detector (deg)
1.	82.8	1.8 to 3
2.	(-)82.8*	1.8 to 3
3.	75	1.8
4.	70	1.8
5.	78	1.8 to 3
6.	72.5	1.8
7.	65	1.8
8.	65	≈1

*Detector 2 placed in opposite half arc as detector 1. The other detectors may be in either half-arc in the plane which contains the E field of the incident beam.

Note that the angular width cannot be large for the detectors placed with $\theta \leq 75$ deg since otherwise they will not resolve the coarse features for the larger of the anticipated bubble size. It is assumed that these detectors will not all be needed for the smaller of the bubbles sizes so that it is not important to average over the fine structure of a small bubble for detectors with $\theta \leq 70$ deg. All of detectors 5-8 are not essential if detectors 1-4 are available.

6. Corrections to the POA--

The POA prediction that the average value I_2 (82.8 deg) ≈ 0.25 begins to break down for very large ka. This is evident by inspection of Fig. 5(a). Hence it will be necessary to include some slowly varying function of ka as a correction factor in the right-hand-side of Eq. (3). This factor may be determined from Mie theory. The physical reasons for this breakdown at large ka are discussed in Langley-Marston (Applied Optics, 1984). The aforementioned correction factor should not significantly affect ability to use either the procedure outlined above nor the modified procedure listed below.

Furthermore, because of the finite angular width of the detectors and approximations intrinsic to the POA, the oscillations of the corresponding detector outputs will be somewhat less than those displayed in Fig. 7-11. This reduction will be most significant at the larger values of ka and the smaller values of θ since the half-width of the coarse angular quasiperiod becomes similar in magnitude to the detector angular width. This is evident from inspection of Fig. 3-5. In a first approximation, it should be possible to account for this reduction by integrating the Mie result over the full angular width of the aperature; however, this procedure assumes the effects of vignetting may be neglected. See item 6 of my letter of April 25. For a discussion of the significance of vignetting on the measurement of an

object's angular spectrum (in this case the scattering pattern of a bubble) see J. W. Goodman, Introduction to Fourier Optics (McGraw-Hill, 1968) Figure 5-6 et. seq.

B. The Value and Use of the Absolute Magnitude of the Voltage Output of the Detector Placed at 82.8°

1. Introduction--

In general, the voltage output of a detector should be of the form

$$v_j(\theta,t) = C(\theta,j)\exp[-r^2(t)/b^2]I_j(\theta)a^2 \qquad (4)$$

where b is a beam radius parameter for the Gaussian beam, r(t) is the time dependent distance of the center of the bubble from the axis of the Gaussian beam, I_j is the normalized irradiance as discussed previously, and $C(\theta,j)$ (which is proportional to the laser power) is determined during system calibration. It is assumed that the bubble radius a is much smaller than the beam radius b. For a given event the v_j takes on their maximum value when r(t) is minimized; call this minimum r(t) the impact parameter for this event y. Hence y is the smallest value of the distance of the center of the bubble from the center of the beam as the bubble drifts through the beam. Note that as in Fig. 1 $r(t_{max}) = y$. The problem is that y is not known!

As shown below the value of $v_j(\theta, t_{max}) \equiv v_j(\theta)$ may be used to simplify the inversion procedure proposed in Sec. A.4 of this Report. It may also be used to check the final size distribution.

2. Simplified Inversion Procedure Based on the Value of v_2 (82.8 deg)--

According to the POA, I_2 (82.8 deg) = 0.25 so that Eq. (4) gives

$$[v_2(82.8 \text{ deg})]/0.25\ C \equiv (a_{min})^2 = \exp(-y^2/b^2)\, a^2, \qquad (5)$$

Note that if y = 0, $a = a_{min}$ but that generally $a \geq a_{min}$ so that from the experimental value for v_2 (and calibration data) a minimum size for the bubble may be

determined. This value should be computed for each event used to eliminate some of the possible roots illustrated in Fig. 7. Thus, for example, we could rule out the roots labeled A_1 and A_2 if $ka_{min} \geq 900$ so that we need only determine which of A_3 or A_4 is the appropriate rot from data on $v_2(\theta)$ for other θ. Similar arguments could be applied to case B shown in Fig. 7. These decision making processes could be done by a computer based algorithm.

3. Use of v_2 (82.8 deg) and the Empirical Bubble Radius a to Define a Sample Volume--

The procedure outlined in Sec. A4 and B2 may be applied on an event-by-event basis to determine the relative concentrations of bubbles of different radii within some radius interval, for example, $\Delta a = 10\ \mu m$. Call this concentration n(a) = bubbles per Δa. Let T be the time duration for the accumulation of this set of event data, for example, we may take T = 60 sec. Suppose, however, it is desired to know the absolute bubble concentration N(a) = bubbles per Δa per volume of water. It is evident that

$$N(a) = n(a)/V, \tag{6}$$

where V is the volume of water swept through the viewed area during the time interval T of this data sample. During this time interval we suppose that the average water velocity u, measured relative to the detector housing, is known. Let y_{max} denote the maximum impact parameter for a detected bubble. This number influences the viewed volume as noted below. Let L denote the length of beam viewed by the detector located at 82.8 deg. It will be assumed that $L >> y_{max}$ and $L >> b$ where b is the Gaussian beam parameter as in Eq. (5). Then the volume of water viewed during this time interval is approximately

$$V \approx (2\, y_{max}\, L)\, uT\, |\sin\psi|, \tag{7}$$

where ψ is the angle between u and the axis of the laser beam. For example, if the background flow velocity is perpendicular to the laser beam $\psi = 90$ deg, Eq. (7) may also contain small geometric correction factors which depend on (y_{max}/L) and on sin(82.8 deg).

One difficulty with the spectrometer of the Wyatt Technology design (for the present application) is that the viewed area ($2\, y_{max}\, L$) may not be well defined. This difficulty was avoided by Gowing and Ling by use of an optical mask to define the sample area. Others, including myself, have proposed the use of coincidence techniques. Unfortunately, none of these techniques are easy to put into effect.

I will assume that L is known (via Wyatt's optics) and that the problem reduces to determining the effective beam half-width y_{max}. Inspection of Eq. (5) shows that the impact parameter for a given event is

$$y = b[2 \ln(a/a_{min})]^{1/2}. \qquad (8)$$

We may set y_{max} during the data analysis by discarding all events for which $y > y_{max}$. I assume that the electronics is sufficiently sensitive, and the background noise sufficiently low, that the smallest bubble of interest will trigger an event provided $y \leq y_{max}$. As a check on the data analysis procedure, the y values for the accepted events should be uniformly (and randomly) distributed in the interval $0 \leq y \leq y_{max}$.

4. The Importance of the Laser Power--

I must emphasize again that if the procedures outlined in Sec. B2 and B3 are to be used it is essential that (i) proper calibration data be obtained, and (ii) any fluctuations in the beam power be taken into account by uniformly adjusting the $C(\theta_j)$. I recommend that either laser output power be monitored or the power in the beam dump be measured.

5. Alternate Method of Verifying Proper Operation Based on Convolution with an Effective Response Function--

I have also outlined an operational check based on the distribution of the measured v_2 (82.8 deg) as well as the inferred distribution of the radii a for the sample of events under consideration. This procedure assumes that the impact parameters y are randomly distributed in the interval $0 \leq y \leq y_{max}$. The procedure makes use of an effective response function which corresponds to the distribution of a_{min}, from Eq. (5), which you would have if the bubbles were all of the same size. This distribution function $g(a_{min}/a)$ may be calculated from first principles if y_{max} is known. Let the number density for the distribution of the a_{min} (in a sample with random values of a) be given by $\tilde{n}(a_{min})$. Then we expect that $\tilde{n}(a_{min})$ should be given by a convolution of n(a) with g. Note that in the special case of a monodispersion of radius a_0, $n(a) \propto \delta(a - a_0)$ where δ is a Dirac δ function. Then the convolution gives $\tilde{n}(a_{min}) \propto g(a_{min}/a_0)$ as expected. In principle it may be possible to determine n(a) from $\tilde{n}(a_{min})$ by a deconvolution procedure but the details have not been examined.

Report Distribution List

R. Hollman — 1 copy
Code 331
Naval Ocean Research and Development Activity
NSTL Station, MS 39529-5004

Ming-Yang Su — 2 copies
Code 331
Naval Ocean Research and Development Activity
NSTL Station, MS 39529-5004

Dr. Logan Hargrove — 1 copy
Physics Division, Code 1112
Office of Naval Research
800 N. Quincy Street
Arlington, VA 22217-5000

ONR, Resident Representative — 1 copy
University of Washington
315 University District Bldg.
1107 N.E. 45th St.
Seattle, WA 98105-4631

Defense Technical — 12 copies
Information Center,
Bldg. 5, Cameron Station
Alexandria, VA 22314

Director, Naval Research — 6 copies
Laboratory, ATTN: Code 2627
Washington, D.C. 20375

Kevin L. Williams — 1 copy
Code 4120
Naval Coastal Systems Center
Panama City, FL 32407-5000

Stuart C. Billette — 1 copy
Bldg. E1, M/S F187
Hughes Aircraft Co.
El Segundo, CA 90245

Prof. L. A. Crum — 1 copy
Dept. of Physics and Astronomy
University of Mississippi
Oxford, MS 38677

Phil Wyatt — 1 copy
Wyatt Technologies
P.O. Box 3003
Santa Barbara, CA 93130

Cleon E. Dean, Dept. of Physics — 1 copy
Washington State University
Pullman, WA 99164-2814

END

1-87

DTIC